

1 **Design and synthesis of Mannich base-type derivatives containing imidazole and**
2 **benzimidazole as lead compounds for drug discovery in Chagas Disease**

3
4 Iván Beltran-Hortelano^{1,2}, Richard L. Atherton³, Mercedes Rubio-Hernández^{1,2}, Julen Sanz-
5 Serrano⁴, Verónica Alcolea^{1,2}, John M. Kelly³, Silvia Pérez-Silanes^{1,2*} and Francisco Olmo^{3*}

6
7 ¹Universidad de Navarra, ISTUN Instituto de Salud Tropical, Irunlarrea 1, 31008, Pamplona,
8 Spain.

9 ²Universidad de Navarra, Pharmacy and Nutrition Faculty, Department of Pharmaceutical
10 Technology and Chemistry, Campus Universitario, 31080, Pamplona, Spain

11 ³Department of Infection Biology, London School of Hygiene and Tropical Medicine, London
12 WC1 7HT, United Kingdom.

13 ⁴Universidad de Navarra, Pharmacy and Nutrition Faculty, Department of Pharmacology and
14 Toxicology, Irunlarrea 1, 31008, Pamplona, Spain.

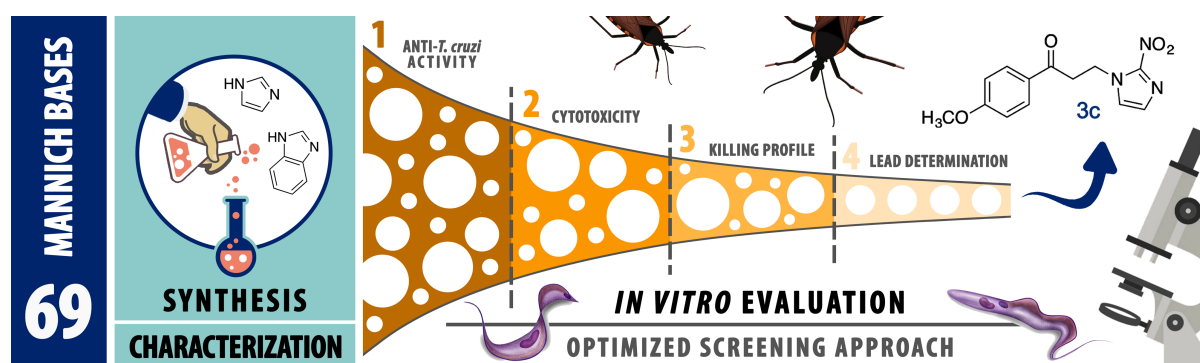
15
16 *corresponding authors

17 Francisco Olmo. Department of Infection Biology, London School of Hygiene and Tropical
18 Medicine, London, United Kingdom. email: Francisco.Olmo@lshtm.ac.uk

19 and

20 Silvia Pérez-Silanes. Universidad de Navarra, Pharmacy and Nutrition Faculty, Department of
21 Pharmaceutical Technology and Chemistry, Campus Universitario, 31080, Pamplona, Spain.
22 email: sperez@unav.es

23
24 **GRAPHICAL ABSTRACT**



28 **ABSTRACT**

29 The protozoan parasite *Trypanosoma cruzi* is the causative agent of Chagas Disease, the most
30 important parasitic infection in Latin America. The only treatments currently available are nitro-
31 derivative drugs that are characterised by high toxicity and limited efficacy. Therefore, there is
32 an urgent need for more effective, less toxic therapeutic agents. We have previously identified
33 the potential for Mannich base derivatives as novel inhibitors of this parasite. To further explore
34 this family of compounds, we synthesized a panel of 69 new analogues, based on multi-
35 parametric structure-activity relationships, which allowed optimization of both anti-parasitic
36 activity, physicochemical parameters and ADME properties. Additionally, we optimized our *in*
37 *vitro* screening approaches against all three developmental forms of the parasite, allowing us to
38 discard the least effective and trypanostatic derivatives at an early stage. We ultimately
39 identified derivative **3c**, which demonstrated excellent trypanocidal properties; both its
40 druggability and low-cost production make this compound a promising candidate for the
41 preclinical, *in vivo* assays of the Chagas disease drug-discovery pipeline.

42

43 **KEYWORDS:** Mannich bases, imidazole, benzimidazole, Chagas disease, neglected tropical
44 diseases, *Trypanosoma cruzi*.

45

46 **HIGHLIGHTS:**

- 47 • Imidazole and benzimidazole Mannich bases as new candidates against Chagas disease.
- 48 • Efficient screening strategy for the evaluation of new 69 Mannich bases against *T.*
49 *cruzi*.
- 50 • A 2'-nitroimidazole derivative identified as candidate to block the infection *in vitro*.
- 51 • The 2'-nitroimidazole **3c** synergizes with benznidazole in combinatory therapy *in vitro*.

52

53 1. Introduction

54 Chagas disease (CD) is the main parasitic infection in Latin America. It is caused by the
55 protozoan *Trypanosoma cruzi*, which is transmitted to humans by triatomine insect vectors. [1].
56 About 6-8 million people are currently infected and more than 70 million people are at risk of
57 acquiring the disease. Unfortunately, less than 1% of people infected with *T. cruzi* have access
58 to diagnosis and treatment [2]. Other modes of transmission (congenital, blood transfusions,
59 organ transplants, and ingesting contaminated food or drink), as well as global migratory
60 movements, have spread CD to previously unaffected regions and continents. To date, there are
61 only two available treatments, benznidazole (BZ) and nifurtimox (NFX). Both are close to
62 100% effective if given soon after infection, but they are not approved for use against the
63 symptomatic chronic form of the disease. Additionally, both drugs have drawbacks, with long
64 treatment periods (60-90 days) and dose-dependent toxicity leading to high drop-out rates
65 amongst patients [2-4]. Novel alternative approaches proposed and developed by groups such as
66 the Drugs for Neglected Diseases *initiative* (DNDi), include new candidate compounds and
67 modifications of existing drug regimens (lower doses, shorter treatment durations and
68 combinations). A new BZ monotherapy regimen, BZ/fosravuconazole combination therapy, and
69 clinical trials of fexinidazole are examples of this [2]. However, despite these efforts, more
70 effective new drugs that are cheaper, safer and more effective than BZ and NFX, have yet to be
71 found [5].

72 Many compounds have been shown to have biological activity against *T. cruzi*, as demonstrated
73 in our previous research [6]. Of note are the arylamine Mannich base-type derivatives, a family
74 of compounds with the ability to inhibit the iron-containing superoxide dismutase (Fe-SOD).
75 The trypanosomatid isoform of this metalloenzyme, which uses iron as cofactor, is not
76 commonly found in eukaryotes [6]. In addition, this group of compounds display other
77 interesting biological activities, including analgesic, anti-bacterial, anti-cancer, anti-convulsant,
78 anti-fungal, anti-inflammatory, antioxidant and anti-viral properties, among others [7,8]. Thus,
79 Mannich bases represent promising alternatives to current anti-parasitic agents, due to their
80 potential biological activity against parasites responsible for tropical diseases such as
81 trypanosomiasis [9], leishmaniasis [10-12] and malaria [13-16]. Our group has continued this
82 line of research via the incorporation of an array of amine fragments and substituents into the
83 general structure of the Mannich bases [17-20], in an attempt to enhance their anti-chagasic and
84 general anti-parasitic activity.

85 The discovery pipeline for the development of pre-clinical drug candidates can be a lengthy
86 process, with an urgent need to design new, more rapid and efficient methodologies. High-
87 throughput screening (HTS) approaches are being increasingly used in drug discovery against

88 parasitic diseases, such as CD, due to the rapidity of the process, the highly informative data
89 generated, and the excellent reproducibility [21-24]. However, although HTS allows many
90 compounds to be tested simultaneously, they produce a high number of ‘false-positive’ hits.
91 This is mainly due to the lack of detailed assays to properly assess the activity profile of these
92 compounds, for example, discriminating between trypanocidal and trypanostatic properties.
93 Therefore, we have developed an optimized strategy for testing small to medium series of
94 compounds (<100) that allows those with low activity to be discarded early in the discovery
95 cascade, the selection of pre-candidates with confirmed trypanocidal activity, and the synthesis
96 of chemically related compounds using the pre-candidate(s) as scaffolds. This approach
97 introduces a significant reduction in the number of assays, time, materials and costs. The
98 selection process ensures that only promising compounds *in vitro* can be progressed to *in vivo*
99 assays. As the strategy progresses, the assays become more physiologically relevant, providing
100 valuable information on the kinetics of the killing profile of each candidate.

101 Heterocyclic compounds are a widely studied group that have gained relevance in recent years
102 in medicinal chemistry research. Imidazole and benzimidazole rings, in particular, have
103 occupied a notable position in nitrogen-containing heterocyclic chemistry. Benzimidazole is
104 formed by the fusion of imidazole, a five-membered aromatic framework containing two
105 nitrogen atoms, and benzene. Both heterocycles display amphoteric and highly polar properties.
106 Moreover, they can easily form diverse, weak binding interactions with a variety of proteins,
107 enzymes and receptors in biological systems, displaying broad pharmacological properties and
108 applications. These pharmacophores have gained significant importance and have been used for
109 many years to treat parasitic diseases including CD, with several imidazole and benzimidazole
110 derivatives having potent anti-*T. cruzi* activity [25]. We have therefore further explored the
111 potential of these two heterocyclic moieties in the design and development of new candidates
112 against *T. cruzi*. A total of 69 Mannich base-type derivatives containing imidazole and
113 benzimidazole components are presented in this paper as novel candidates against *T. cruzi*. Our
114 work also introduces a new *in vitro* screening strategy, which has allowed rapid and efficient
115 evaluation of this small library of compounds.

116

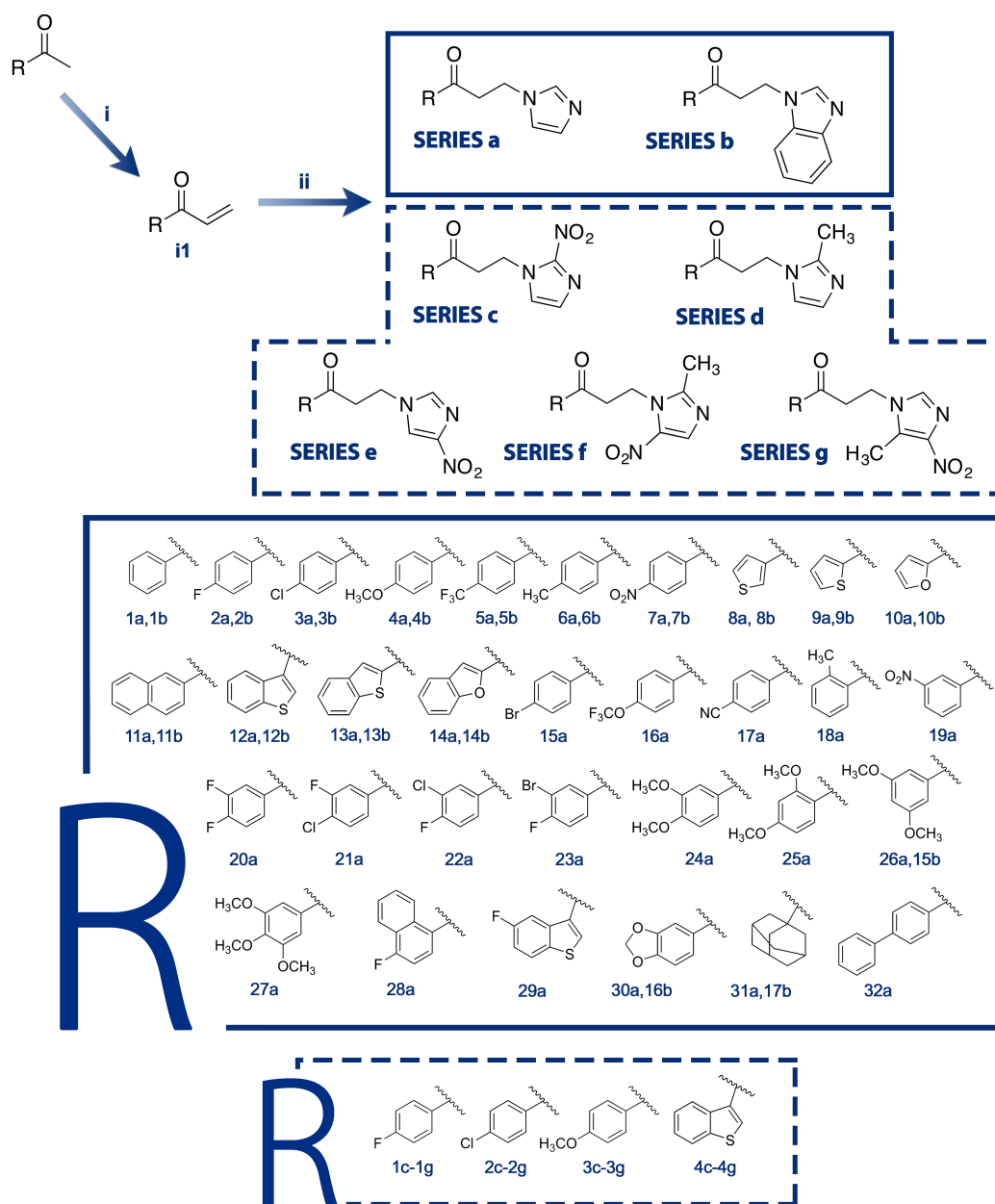
117 **2. Results and discussion**

118 **2.1 Chemistry**

119 Based on our group’s previous experience in the synthesis of trypanocidal compounds [17-20],
120 we focused our attention on Mannich base derivatives as their synthesis pathways are simple,
121 cost-effective and make use of commercially available chemical reagents. The precise route of
122 synthesis chosen is outlined in **Scheme 1**, in which the vinyl ketone (**11**) was obtained from the

123 corresponding methyl ketone (commercially available) using a diisopropylammonium 2,2,2-
124 trifluoroacetate catalyst and paraformaldehyde, in tetrahydrofuran (THF), under reflux and
125 acidic conditions [26]. The following step describes the condensation of the
126 imidazole/benzimidazole ring (**ii**) with the previously synthesised vinyl ketone, via a Michael
127 addition reaction at room temperature.

128 IR, ^1H NMR and ^{13}C NMR spectroscopic data, elemental microanalysis (C, H, N) and
129 electrospray ionisation mass spectra (MS-LC TOF), were required for the full characterisation
130 of all of these new derivatives, as detailed in the **Experimental section**. In some cases, for an
131 accurate assignment of the signals in the ^1H and ^{13}C NMR spectra, which were registered in
132 deuterated dimethylsulfoxide ($\text{DMSO-}d_6$), DEPT-135 and heteronuclear simple quantum
133 coherence (gHSQC) experiments were performed.



134

135 **Scheme 1. Reagents and conditions for the synthesis of 69 Mannich base derivatives:** (i)
 136 paraformaldehyde, diisopropylammonium 2,2,2-trifluoroacetate, trifluoroacetic acid, THF, reflux, 8 h; (ii)
 137 THF, K₂CO₃, rt, from 24 to 72 h.

138

139 **2.2 Killing profile of the lead compounds: IC₅₀, SI determination and kinetics of**
 140 **epimastigote killing**

141 Preliminary screening allowed us to select 8 lead compounds (**7a**, **18a**, **19a**, **21a**, **28a**, **15b**, **17b**
 142 and **3c**) (see **Supplementary section**), which showed activity against *T. cruzi* CL-Luc:Neon
 143 clone epimastigotes [27] and limited toxicity to BSR mammalian cells, from an initial library of
 144 69 nitroheterocyclic derivatives. Their IC₅₀ and SI values against epimastigotes and BSR cells
 145 were then determined (**Table 1**) according to the methodology described in the **Experimental**

146 **section.** Compound **3c** was the most promising candidate, with a lower IC₅₀ value than BZ. We
 147 also followed the growth rate of drug-exposed parasites in real time by monitoring fluorescence
 148 for 7 days (**Experimental section**). Reference drug BZ is considered “fast-killing”, as a single
 149 dose can decrease the parasitaemia drastically in 24 h in animal models [28]. Consistent with
 150 this, at all effective BZ concentrations (>2.5 μM), parasite growth had dropped by day 3 of the
 151 treatment (**Figure 1A**). A similar profile was shown by derivative **3c** (**Figure 1B**).

152 **Table 1.** IC₅₀ values (μM) for inhibition of the growth of *T. cruzi* CL-Luc:Neon clone epimastigotes and
 153 for the cytotoxicity toward BSR host cells of selected compounds. **BZ** has been included as a reference
 154 drug. Data are presented as the mean ± SD of triplicates of three independent experiments after 72 h
 155 exposure. Yellow shading highlights compounds selected for further evaluation.

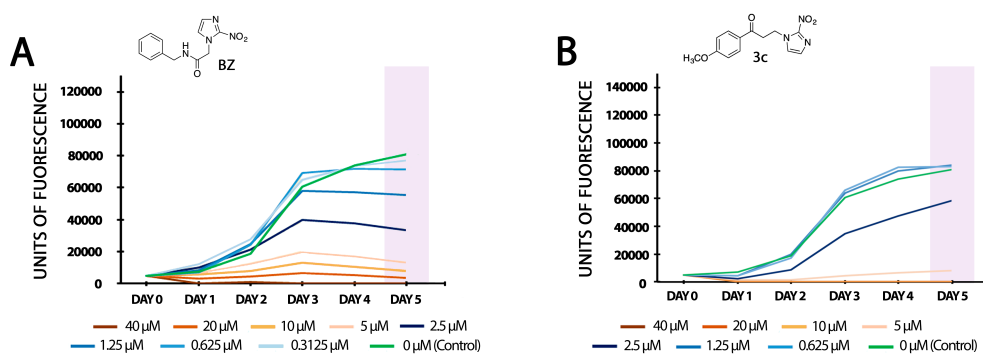
156

| Compound | IC ₅₀ (mean ± SD), μM | | Selectivity Index (SI) |
|------------|----------------------------------|--------------------|------------------------|
| | Epimastigotes | BSR Cells | |
| 7a | 12.9 ± 1.8 | 93.9 ± 1.9 | 7 |
| 18a | 21.4 ± 1.2 | 144.6 ± 5.8 | 7 |
| 19a | 21.6 ± 4.0 | 177.4 ± 1.8 | 8 |
| 21a | 23.3 ± 4.9 | 134.6 ± 2.7 | 6 |
| 28a | 7.4 ± 0.5 | 72.2 ± 1.2 | 10 |
| 15b | 11.1 ± 3.2 | 70.1 ± 9.6 | 6 |
| 17b | 24.8 ± 5.8 | 67.6 ± 6.1 | 3 |
| 3c | 2.2 ± 0.6 | 84.7 ± 1.2 | 43 |
| BZ | 3.8 ± 0.7 | 267.3 ± 1.3 | 67 |

157

158

159



160

161 **Figure 1.** Kinetics of growth inhibition of *T. cruzi* CL-Luc:Neon clone epimastigotes over time in the
 162 presence of **BZ** (A) and compound **3c** (B). Data are presented as units of fluorescence, obtained by real
 163 time fluorescence readout for 5 days, by which time epimastigotes had reached the stationary phase.

164

165 2.3 Drug-like Properties

166 Employing the Molinspiration [29] and Osiris Data Warrior [30] software, compounds (**7a**, **19a**,
 167 **28a** and **3c**) were analysed to predict their physiochemical properties, in relation to absorption

168 and bioavailability (**Table 2**). None of the derivatives, including BZ, violated the Lipinski's rule
 169 of five [31]. It has been well established that optimal lipophilicity range, along with low logP
 170 (<5) and low topological polar surface area (TPSA), are the major driving forces that lead to
 171 good absorption, including intestinal absorption, bioavailability, Caco-2 cell permeability, and
 172 blood-brain barrier penetration. Molecules with a TPSA of <140 Å² are indicative of excellent
 173 bioavailability [32]. The calculated logP and TPSA values for derivatives **7a**, **19a**, **28a** and **3c**
 174 range from 0.12 to 2.51, suggesting that these compounds should be able to cross cell
 175 membranes. This was confirmed by their ability to kill epimastigotes.

176 The drug score combines drug likeness, logP, molecular weight and toxicity risks in one handy
 177 value that can be used to infer therapeutic potential. A value of >0.5 indicative of theoretical
 178 promise as a safe and efficient drug [33]. Compounds **3c** had the highest drug score (0.61)
 179 among the evaluated compounds. For comparison, the BZ displays a drug score of 0.33.

180

181 **Table 2.** Theoretical molecular properties for selected compounds **7a**, **19a**, **28a** and **3c**.

| Molecular Properties (Molinspiration and Osiris Calculations) | | | | | | | | | | |
|---|--------|-------|-------|-------|-----------|------------|----|--------|------------|---------------|
| Compound | MW | cLogP | cLogS | TPSA | H Acep | H Donor | NV | Vol | Drug LK | Drug Score |
| 7a | 245.24 | 0.12 | -2.15 | 80.72 | 6 | 0 | 0 | 212.58 | -1.35 | 0.57 |
| 19a | 245.24 | 0.12 | -2.15 | 80.72 | 6 | 0 | 0 | 212.58 | -1.35 | 0.57 |
| 28a | 268.29 | 2.51 | -3.61 | 34.89 | 3 | 0 | 0 | 238.17 | 2.43 | 0.43 |
| 3c | 275.26 | 0.42 | -2.43 | 89.95 | 7 | 0 | 0 | 238.13 | -2.55 | 0.61 |
| BZ | 260.25 | 0.12 | -2.15 | 92.75 | 7 | 1 | 0 | 224.99 | -1.71 | 0.33 |

182

183 **2.4 IC₅₀ and SI determination against amastigotes and trypomastigotes.**

184 We also evaluated the ability of compounds **7a**, **19a**, **28a** and **3c** to inhibit the replication of
 185 intracellular amastigotes (**Table 3**). Amastigotes are the most clinically relevant life-cycle stage
 186 in the mammalian host. Effective drugs must be able to cross the host cell membrane to act
 187 against the parasite. The IC₅₀ values, which were calculated after 3 days exposure (see
 188 **Experimental section**), revealed that derivatives **28a** and **3c** were similarly effective against
 189 both epimastigotes and amastigotes. In contrast, compounds **7a** and **19a** were more effective
 190 against amastigotes, although the IC₅₀ values were still relatively modest, at 9.1 and 12.2 μM,
 191 respectively.

192 Non-replicative trypomastigotes are the parasite forms responsible for cellular invasion, as well
 193 as the form taken up by the insect vectors in a blood meal from an infected host. We tested the
 194 selected compounds against this flagellated extracellular form (**Experimental section**).
 195 Compounds **28a** and **3c** were the most active derivatives, with IC₅₀ values of 16.6 and 9.1 μM,

196 respectively, even more active than BZ (22.4 μ M). Compound **19a** displayed similar activity to
 197 the reference drug. In contrast, derivative **7a** was inactive against this parasitic form and
 198 discarded from future assays.

199

200 **Table 3.** IC₅₀ values (μ M) against *T. cruzi* amastigotes and trypomastigotes of compounds **7a**, **19a**, **28a**
 201 and **3c**. **BZ** was included as a reference drug. Data are presented as the mean \pm SD of triplicates of three
 202 independent experiments after 72 h of incubation. nd, non-determined.

203

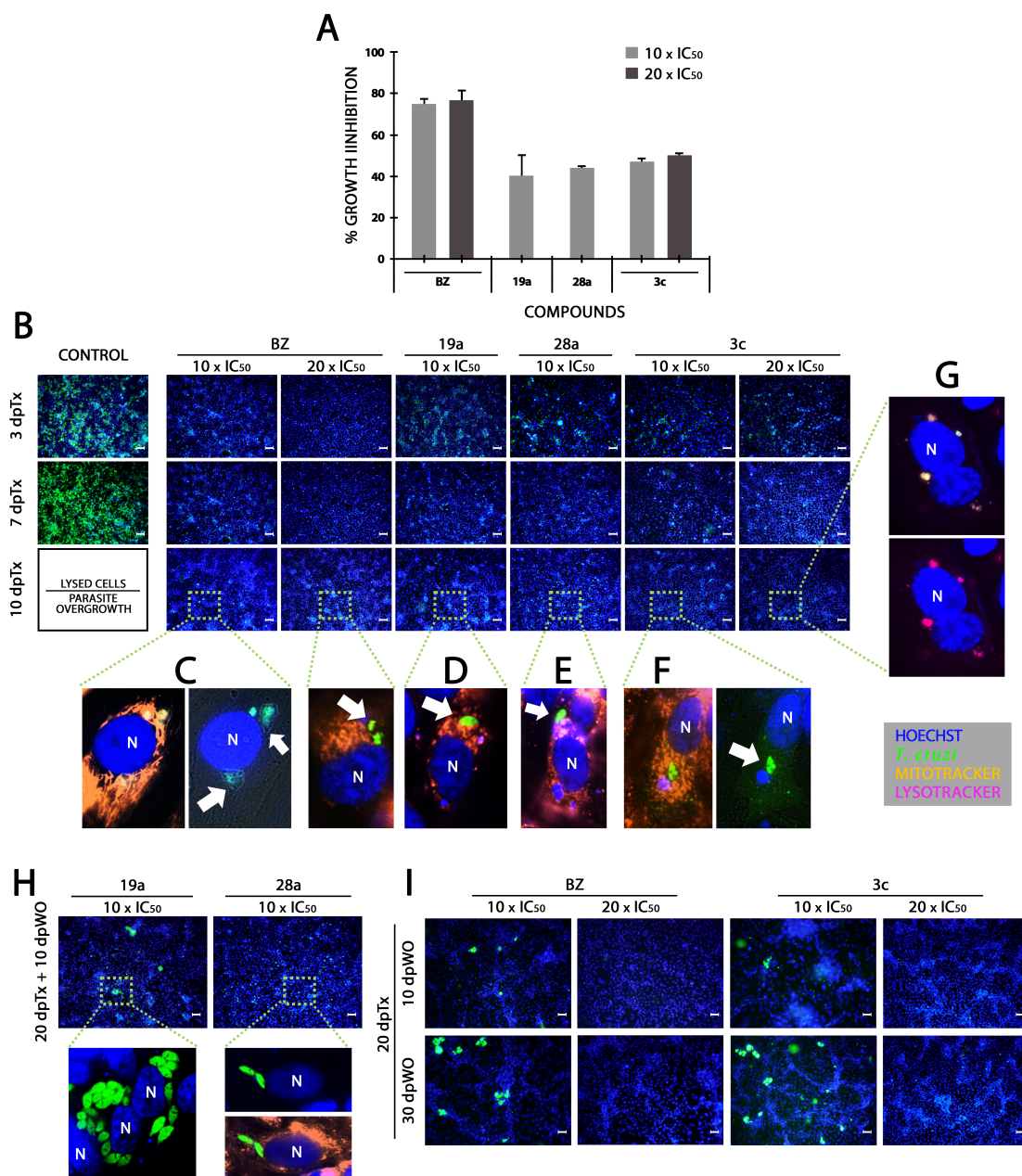
| Compound | IC ₅₀ (mean \pm SD), μ M | | | Selectivity Index (SI) | |
|------------|---|-----------------|-----------------|------------------------|-----------------|
| | Amastigotes | Trypomastigotes | BSR Cells | Amastigotes | Trypomastigotes |
| 7a | 9.1 \pm 0.6 | nd | 93.9 \pm 1.9 | 10 | nd |
| 19a | 12.2 \pm 1.7 | 23.0 \pm 1.0 | 177.4 \pm 1.8 | 15 | 8 |
| 28a | 6.1 \pm 1.6 | 16.6 \pm 0.3 | 72.2 \pm 1.2 | 12 | 4 |
| 3c | 3.3 \pm 1.3 | 9.1 \pm 2.3 | 84.7 \pm 1.2 | 28 | 9 |
| BZ | 0.5 \pm 0.1 | 22.4 \pm 3.5 | 267.3 \pm 1.3 | 504 | 12 |

204

205 **2.5 Wash-out Assays**

206 To fully understand the activity profile of compounds **19a**, **28a** and **3c**, we undertook wash-out
 207 assays, modifying a protocol described by Cal *et al.* [34] (**Experimental section**). The
 208 usefulness of this assay has become more apparent since the advent of high-throughput
 209 screening technologies. It allows viable persistent parasites that survive treatment, because of
 210 their reduced drug susceptibility, to be identified [35]. This assay provides an early insight into
 211 the potential for compound failure, before their use in animal models. In the wash-out assay,
 212 parasite-infected cells were exposed to high test compound concentrations (10 and 20 x IC₅₀) for
 213 either 10 or 20 days, after which the compound was removed from the culture medium. Infected
 214 and treated cultures were then monitored by fluorescent microscopy for a further 30 days after
 215 removal of the drugs, to investigate parasite relapse (**Figure 2**). By day 3 post-treatment, there
 216 was growth inhibition (**Figure 2A**). However, in all cases where less than 10 x IC₅₀ treatment
 217 conditions were used, renewed parasite growth was detectable, regardless of whether initial
 218 exposure was for 10 or 20 days. In the case of derivatives **19a** and **28a**, where due to host cell
 219 toxicity, we could only use the 10 x IC₅₀ concentration, intact parasites could still be seen after
 220 10 days treatment (**Figure 2B-D**). Even with 20 days exposure, dividing parasites were
 221 detectable 10 days after compound removal (**Figure 2H**), indicative of a trypanostatic mode of
 222 action for these derivatives. By contrast, both the reference drug BZ and compound **3c** could be
 223 inferred to have a strong trypanocidal effect when given for 20 days at the 20 x IC₅₀
 224 concentration. By day 10 post-exposure, this type of trypanocidal profile was already visible,

225 with apparently destroyed parasites, some of which were broken up, and others already taken
 226 into the lysosomal pathway of host cells for degradation (**Figure 2F**). Even 30 days after drug
 227 removal (**Figure 2I**), the BZ and compound **3c** cultures remained clear of parasites.
 228 Collectively, these results confirm that **3c** can eliminate *T. cruzi* intracellular stages, without the
 229 survival of persistent parasites.

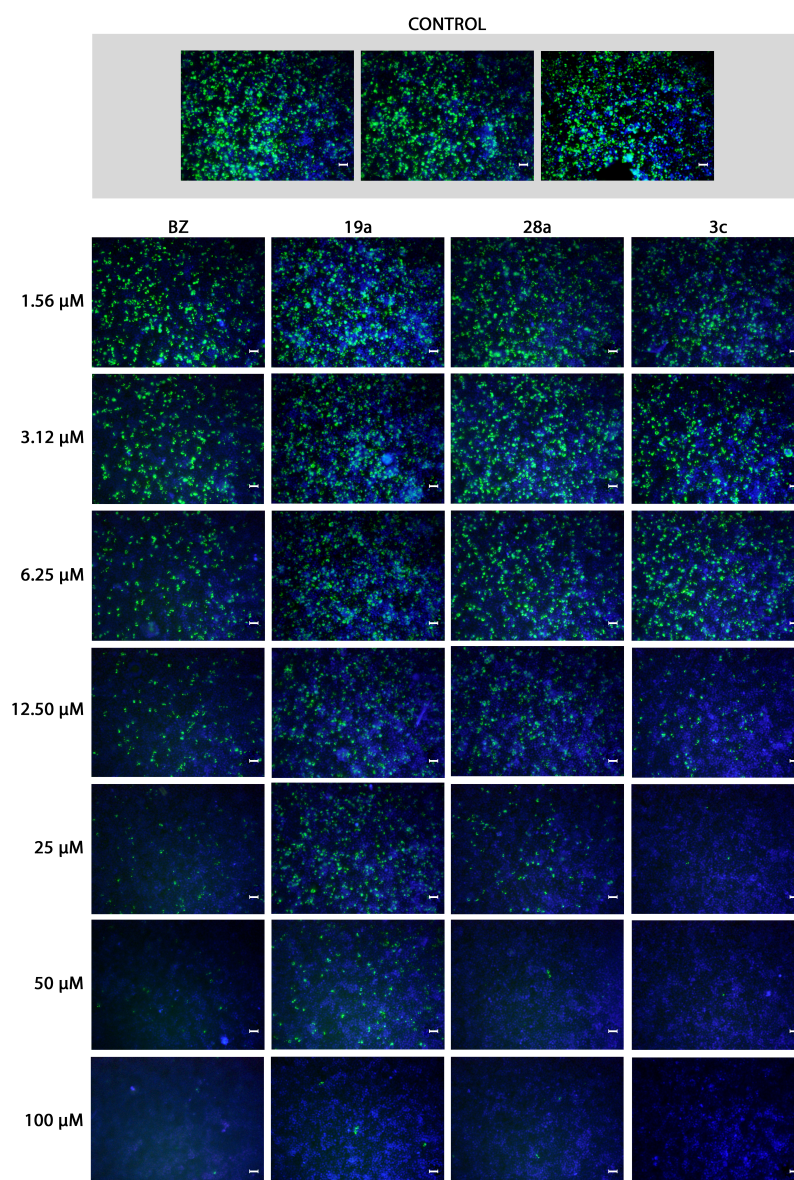


230
 231 **Figure 2.** Wash-out assays for **BZ** and derivatives **19a**, **28a** and **3c** against *T. cruzi* CL-Luc:Neon clone
 232 amastigotes in BSR infected cells. **A**, Growth inhibition after 72 h treatment measured as fluorescent
 233 intensity compared to untreated group. **B**, Representative fields (of 30 captures per treatment) from the
 234 treated wells under epifluorescence microscopy at different timepoints post-treatment. **C**, **D**, **E**, **F**, **G**, **H**
 235 and **I**. Representative zoomed areas of interest under different treatments visualised by epifluorescence
 236 microscopy. Cell dyes (mitotracker and lysotracker) are used for a better location of parasites in the
 237 intracellular domain. dpTx, days post-treatment; dpWO, days post drug wash-out. N, mammalian cell
 238 nuclei. White arrows indicate parasites. Scale bars = 50 μ m.

239

240 **2.6 Infectivity assay**

241 Trypomastigotes are often more refractory to drug treatment than the replicating amastigote
242 form, which is consistent with the obtained IC₅₀ values (**Table 3**). For these assays, we
243 determined the drug concentrations that reduced trypomastigote infectivity by 50% compared to
244 untreated control. We also sought to determine the minimal concentration of drug required to
245 produce a sterile infection following 6 h incubation with trypomastigotes. Using fluorescence
246 microscopy, we found that pre-exposure to **3c** at concentrations >50 μ M completely blocked
247 trypomastigote infectivity. In contrast, even at BZ concentrations >100 μ M, some persistent
248 parasites were observed 5 days post-infection (**Figure 4**). Whether the impact of **3c** on infection
249 was due to trypomastigotes being killed directly by drug action, or by damage that prevents
250 them infecting host cells remains unknown.



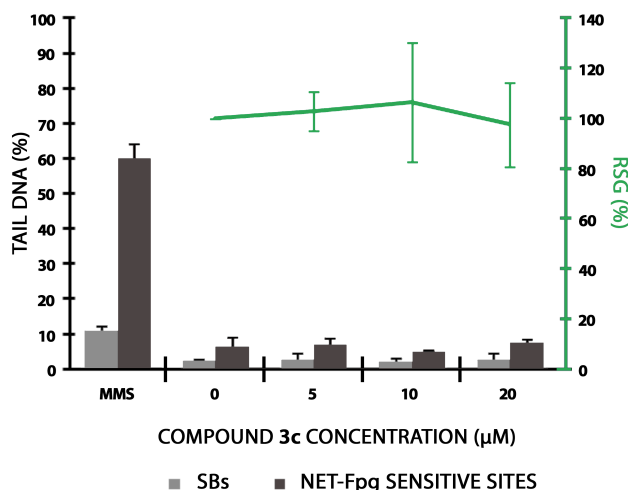
251

252 **Figure 4.** Infectivity assays of *T. cruzi* CL-Luc:Neon trypomastigotes pre-treated with **BZ** or derivatives
253 **19a**, **28a** and **3c** for 6 h prior to infection of BSR cells (Experimental section). Values were established
254 from amastigote fluorescence 5 days post-infection. Images of broad field captures are shown at 20x
255 under epifluorescence microscopy for increasing drug concentrations. These are representative of 30
256 images taken per treatment. Host-cell nuclei are shown in blue (DAPI staining), with parasites in green;
257 scale bars = 50 μ m.
258
259
260

261 **2.7 In vitro toxicity screening: Comet Assay**

262 The formamide pyrimidine DNA glycosylase (Fpg)-modified comet assay was performed to
263 check the potential genotoxic effect of derivative **3c** on human cells. To do so, we used the
264 human lymphoblastoid TK-6 cell line, which is widely used in genotoxicity testing since they
265 are p53-competent (recommended by several OECD guidelines for *in vitro* genotoxicity and
266 mutagenicity assays).
267

268 This version of the assay detects both DNA strand breaks (SBs) and oxidised/alkylated bases
269 [36,37]. To prevent a misinterpretation of the comet assay readout due to widespread DNA
270 degradation induced by lethal doses, we simultaneously ran a proliferation assay. The latter acts
271 to confirm cell integrity. DNA damage associated with cells under conditions where
272 proliferation is inhibited by >25 % is considered a false positive outcome with the comet assay.
273 **Figure 5** shows the results obtained in the Fpg-modified and the proliferation assays after 3 h of
274 treatment. A 46% decrease in proliferation was observed in TK-6 cells treated with 40 μ M **3c**
275 (data not shown), and for the reasons explained, comet assays were not performed at
276 concentrations up to and beyond this limit. For all the concentrations below, the levels of SBs
277 and Fpg-sensitive sites were not significantly different ($p>0.05$) from the untreated controls. In
278 contrast, analysis of cells treated with 20 μ M of the DNA alkylating agent MMS (methyl
279 methanesulphonate), which were included a positive control, revealed extensive genotoxic
280 damage (**Figure 5**). Collectively, these results are consistent with a safe profile for compound
281 **3c**, in terms of DNA damage, over the concentration range at which it is therapeutically active
282 against the different forms of *T. cruzi*.
283

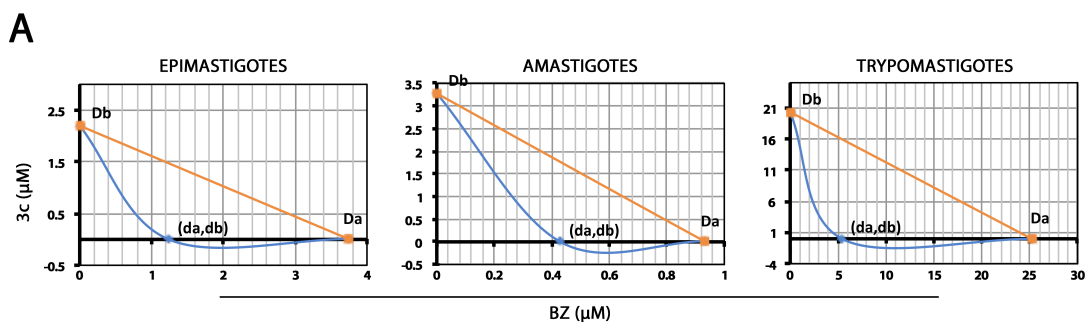


284
285

286 **Figure 5.** Comet and proliferation assays performed on **3c**-treated TK-6 cells after 3 h exposure. SBs and
 287 Net-Fpg sensitive sites are represented as a percentage of the DNA in the comet's tail relative to the DNA
 288 remaining in the comet. SBs and Fpg-sensitive sites were not statistically different under all conditions
 289 tested when compared to control values ($p > 0.05$). For the proliferation assay, cells were washed after the
 290 treatment and cultured for 48 h. Cells were then counted and the relative suspension growth (RSG) was
 291 calculated (Experimental section) in relation to the untreated control. Results are presented as the mean \pm
 292 SD of triplicates of three independent experiments. MMS-treated cells (20 μ M) were included as a
 293 positive control for DNA damage.
 294

295 2.7 Drug combination assay

296 Whilst BZ is effective in long regimens, toxicity is a major reason for low rates of compliance,
 297 which ultimately leads to treatment failure. There is a strong rationale to search for compounds
 298 that in combination with BZ can allow its dosage and/or treatment period to be reduced, while
 299 obtaining similar curative rates. The trypanocidal effect of derivative **3c** against
 300 trypomastigotes, with activity greater than BZ, encouraged us to undertake a combinatory assay.
 301 The results (**Figure 6**) showed a synergic effect of **3c** on the BZ IC_{50} . While this effect was
 302 minimal against intracellular forms, it was prominent against both extracellular forms. In the
 303 case of the epimastigotes (insect vector forms), **3c** decreased the BZ IC_{50} by almost 70%, in
 304 comparison with a single treatment of BZ. The synergic effect was even greater in the case of
 305 trypomastigotes (mammalian infective forms), where the IC_{50} value dropped to almost a quarter
 306 of that obtained for BZ alone.



B

| <i>T. cruzi</i> Form | IC ₅₀ (mean ± SD), μM | | Ci | BZ IC ₅₀ Fold Decreased in Combination |
|----------------------|----------------------------------|-----------|------|--|
| | BZ | BZ + 3c | | |
| Epimastigote | 3.8 ± 0.7 | 1.2 ± 0.1 | 0.33 | 3x |
| Amastigote | 0.5 ± 0.1 | 0.4 ± 0.1 | 0.81 | - |
| Trypomastigote | 22.4 ± 3.5 | 5.4 ± 1.7 | 0.21 | 4x |

307

308

309 **Figure 6.** Drug combination assay. A, isobolograms of concentration-effect curves of **3c** and **BZ** and their
 310 combinations against different developmental forms of *T. cruzi*. B, table showing the variation of BZ IC₅₀
 311 when the assays were performed in the presence of the IC₅₀ concentrations of **3c**; Ci (coefficient of
 312 interaction) shows the synergic relation between drugs (Ci < 1). Data are shown as mean ± SD (n = 3).
 313 Orange lines link the IC₅₀ values for drugs assayed independently (Da, **BZ**; Db, **3c**), while blue lines show
 314 the shift of the IC₅₀ for **BZ** (da) assayed in the presence of **3c** (db).

315

316

317 3. CONCLUSION

318

319 In summary, we synthesised and characterised a total of 69 Mannich base-type derivatives
 320 bearing imidazole and benzimidazole-functionalized cores. *In vitro* cell-based studies
 321 demonstrated that, of these, compound **3c** had the most promising trypanocidal activity across
 322 the distinct life stages of the parasite. It displayed fast-killing activity at low micromolar doses,
 323 lacked host cell genotoxicity, and had a synergistic mode of action against trypomastigotes in
 324 combination with the reference drug BZ.

325

326 4. EXPERIMENTAL SECTION

327 4.1 Chemistry

328 Chemical reagents used for compound synthesis were purchased from: E. Merck (Darmstadt,
 329 Germany); Panreac Química S.A. (Montcada I Reixac, Barcelona, Spain); Sigma-Aldrich
 330 Química S.A. (Alcobendas, Madrid, Spain); Acros Organics (Janssen Pharmaceuticaaan, Geel,
 331 Belgium); abcr GmbH (Karlsruhe, Germany); Fluorochem Ltd. (Hadfield, Derbyshire, United
 332 Kingdom). The progress of all reactions was monitored by thin layer chromatography (TLC)
 333 using SIL G/UV₂₅₄, 0.2mm thickness (ALUGRAM® Xtra SIL G, Macherey-Nagel GmbH & Co.
 334 KG) as the stationary phase, and solvent mixtures (CH₂Cl₂/methanol or hexane/ethyl acetate) as
 335 the mobile phase; UV lamps (254nm) were employed to spots detection. Purification of

336 compounds was carried out on a CombiFlash® RF instrument (Teledyne Isco), employing Silica
337 RediSep Rf Gold® columns in a normal phase gradient. Infrared spectra (IR) were recorded on a
338 Thermo Nicolet FT-IR Nexus spectrophotometer using potassium bromide (KBr) pellets for
339 solid samples. IR absorption peaks signals (cm⁻¹) were expressed as strong (s), medium (m), and
340 weak (w). Proton (¹H) and carbon (¹³C) NMR spectra of every compound were recorded on a
341 Bruker Advance Neo 400 Ultrashield™ spectrometer (Rheinstetten, Germany) operating at
342 400/100 MHz (¹H/¹³C) and using DMSO-*d*₆ as solvent and tetramethylsilane (TMS) as
343 reference. Chemical shifts (δ) were reported in parts per million (ppm), coupling constants (*J*)
344 were given in hertz (Hz) and multiplicities detected in ¹H-RMN. Elemental analysis was
345 performed on a LECO CHN-900 Elemental Analyzer (Leco, Tres Cantos, Spain). Purity of
346 compounds was confirmed when elemental analysis values were within the range of ± 0.4 with
347 respect to theoretical values. Melting points (Mp) were determined on a Mettler FP82 + FP80
348 apparatus (Greifensee, Switzerland). High-resolution mass spectrometry data were obtained
349 using G220 Accurate-Mass TOF LC/MS (time of flight analyzer) and HPLC 1200 series
350 Agilent® Technologies.

351

352 **4.2 General Procedure for the Synthesis of Compounds**

353 *4.2.1 Synthesis of the intermediate compounds (i1)*

354 To a solution of the corresponding methyl ketone reagent (1eq) in THF (10mL), the
355 paraformaldehyde (8eq), diisopropylammonium 2,2,2-trifluoroacetate catalyst (1.5eq) and
356 trifluoroacetic acid (0.1eq) were added. The mixture was stirred at reflux for 8 h. New 8eq of
357 paraformaldehyde were added to the mixture at 2 h and 5 h of the reaction. The reaction was
358 monitored by TLC (hexane/ethyl acetate). Following this, the solvent was removed under
359 vacuum by rotatory evaporation. The residue was diluted in diethyl ether and the corresponding
360 vinyl ketone **i1** was isolated by a triple extraction after addition of HCl 1N (25 mL), NaOH 1N
361 (25 mL) and saturated NaCl solution (25 mL). The organic phase was dried over anhydrous
362 Na₂SO₄, filtered and the solvent was removed under vacuum.

363 *4.2.2 Synthesis of imidazole (1a-31a) and benzimidazole Mannich bases-type derivatives (1b- 364 17b).*

365 The general procedure for the synthesis of all final compounds was carried out by Michael
366 addition reaction between the previously synthesised vinyl ketones (**i1**) and
367 imidazole/benzimidazole.

368 To a solution of **i1** (1eq) in THF (20 mL) was added the corresponding amine (1eq) and K₂CO₃
369 (1.2eq), then stirred at room temperature for 24-72 h. The reaction was monitored by TLC
370 (DCM/methanol). The residue was purified by automated flash chromatography using
371 DCM/methanol gradient solvent. Next, the solvent was removed under vacuum by rotatory

372 evaporation. The residue was diluted in DCM and the corresponding final compounds were
373 isolated by an extraction after addition of water (25 mL x 3 times). The organic phase was dried
374 over anhydrous Na₂SO₄, filtered and the solvent was removed under vacuum. The final
375 compounds were obtained by precipitation with *n*-hexane.

376

377 4.3 Compound Characterisation

378 *3-(1H-imidazol-1-yl)-1-phenylpropan-1-one (1a)*. Yield: 24%. Mp: 96.5-97.5 °C. IR (KBr) ν
379 cm⁻¹: 1679 (s, $\nu_{C=O}$). ¹H NMR (DMSO-*d*₆, 400 MHz) δ ppm: 7.97 (dd, 2H, **H₂+H₆**, $J_{2,3} = J_{6,5} =$
380 8.3 Hz, $J_{2,4} = J_{6,4} = 1.2$ Hz); 7.66 (s, 1H, **H₂**); 7.64 (td, 1H, **H₄**, $J_{4,3} = J_{4,5} = 6.9$ Hz, $J_{4,2} = J_{4,6} = 1.6$
381 Hz); 7.55-7.51 (m, 2H, **H₃+H₅**); 7.21 (s, 1H, **H₅**); 6.86 (s, 1H, **H₄**); 4.33 (t, 2H, **CH₂-N**, $J_{CH_2-CH_2}$
382 = 6.8 Hz); 3.60 (t, 2H, **CH₂-CO**, $J_{CH_2-CH_2} = 6.8$ Hz). ¹³C NMR (DMSO-*d*₆, 100 MHz) δ ppm:
383 197.71 (**CO**); 137.44 (**C₂**); 136.23 (**C₁**); 133.47 (**C₄**); 128.74 (2C, **C₂+C₆**); 128.25 (**C₄**); 127.94
384 (2C, **C₃+C₅**); 119.42 (**C₅**); 41.17 (**CH₂-N**); 39.27 (**CH₂-CO**). Anal. Calc. for C₁₂H₁₂N₂O: C
385 71.98%, H 6.04%, N 13.99%. Found: C 71.78%, H 6.29%, N 13.86%.

386 *1-(4-fluorophenyl)-3-(1H-imidazol-1-yl)-1-phenylpropan-1-one (2a)*. Yield: 26%. Mp: 65.0-
387 66.0 °C. IR (KBr) ν cm⁻¹: 1681 (s, $\nu_{C=O}$), 1226 (s, ν_{C-F}). ¹H NMR (DMSO-*d*₆, 400 MHz) δ ppm:
388 8.06 (dd, 2H, **H₂+H₆**, $J_{2,3} = J_{6,5} = 8.8$ Hz, $J_{2,F} = J_{6,F} = 5.5$ Hz); 7.65 (s, 1H, **H₂**); 7.35 (t, 2H,
389 **H₃+H₅**, $J_{3,2} = J_{5,6} = J_{3,F} = J_{5,F} = 8.8$ Hz); 7.20 (s, 1H, **H₅**); 6.86 (s, 1H, **H₄**); 4.32 (t, 2H, **CH₂-N**,
390 $J_{CH_2-CH_2} = 6.8$ Hz); 3.59 (t, 2H, **CH₂-CO**, $J_{CH_2-CH_2} = 6.8$ Hz). ¹³C NMR (DMSO-*d*₆, 100 MHz) δ
391 ppm: 196.32 (**CO**); 165.16 (d, **C₄**, $^1J = 252$ Hz); 137.42 (**C₂**); 133.00 (d, **C₁**, $^4J = 2.8$ Hz);
392 130.99 (2C, d, **C₂+C₆**, $^3J = 9.5$ Hz); 128.25 (**C₄**); 119.41 (**C₅**); 115.75 (2C, d, **C₃+C₅**, $^2J = 21.9$
393 Hz); 41.13 (**CH₂-N**); 39.23 (**CH₂-CO**). Anal. Calc. for C₁₂H₁₁FN₂O: C 66.05%, H 5.08%, N
394 12.84%. Found: C 65.67%, H 5.37%, N 12.77%.

395 *1-(4-chlorophenyl)-3-(1H-imidazol-1-yl)propan-1-one (3a)*. Yield: 21%. Mp: 105.0-
396 106.0 °C. IR (KBr) ν cm⁻¹: 1680 (s, $\nu_{C=O}$). ¹H NMR (DMSO-*d*₆, 400 MHz) δ ppm: 7.98 (d, 2H,
397 **H₂+H₆**, $J_{2,3} = J_{6,5} = 8.6$ Hz); 7.65 (s, 1H, **H₂**); 7.59 (d, 2H, **H₃+H₅**, $J_{3,2} = J_{5,6} = 8.6$ Hz); 7.20 (s,
398 1H, **H₅**); 6.86 (s, 1H, **H₄**); 4.32 (t, 2H, **CH₂-N**, $J_{CH_2-CH_2} = 6.8$ Hz); 3.59 (t, 2H, **CH₂-CO**, $J_{CH_2-CH_2}$
399 = 6.8 Hz). ¹³C NMR (DMSO-*d*₆, 100 MHz) δ ppm: 196.77 (**CO**); 138.39 (**C₄**); 137.42 (**C₂**);
400 134.89 (**C₁**); 129.88 (2C, **C₂+C₆**); 128.85 (2C, **C₃+C₅**); 128.26 (**C₄**); 119.41 (**C₅**); 41.08 (**CH₂-**
401 **N**); 39.29 (**CH₂-CO**). Anal. Calc. for C₁₂H₁₁ClN₂O: C 61.42%, H 4.72%, N 11.94%. Found: C
402 61.38%, H 4.95%, N 11.91%.

403 *3-(1H-imidazol-1-yl)-1-(4-methoxyphenyl)propan-1-one (4a)*. Yield: 32%. Mp: 76.5-
404 77.5 °C. IR (KBr) ν cm⁻¹: 1669 (s, $\nu_{C=O}$). ¹H NMR (DMSO-*d*₆, 400 MHz) δ ppm: 7.95 (d, 2H,
405 **H₂+H₆**, $J_{2,3} = J_{6,5} = 8.9$ Hz); 7.65 (s, 1H, **H₂**); 7.20 (s, 1H, **H₅**); 7.04 (d, 2H, **H₃+H₅**, $J_{3,2} = J_{5,6} =$
406 8.8 Hz); 6.85 (s, 1H, **H₄**); 4.30 (t, 2H, **CH₂-N**, $J_{CH_2-CH_2} = 6.8$ Hz); 3.83 (s, 3H, **OCH₃**); 3.52 (t,
407 2H, **CH₂-CO**, $J_{CH_2-CH_2} = 6.8$ Hz). ¹³C NMR (DMSO-*d*₆, 100 MHz) δ ppm: 195.98 (**CO**); 163.32

408 (C₄); 137.41 (C₂); 130.29 (2C, C₂+C₆); 129.24 (C₁); 128.23 (C₄); 119.44 (C₅); 113.92 (2C,
409 C₃+C₅); 55.55 (OCH₃); 41.31 (CH₂-N); 38.89 (CH₂-CO). Anal. Calc. for C₁₃H₁₄N₂O₂: C
410 67.81%, H 6.13%, N 12.17%. Found: C 67.84%, H 6.31%, N 12.24%.

411 3-(1*H*-imidazol-1-yl)-1-(4-(trifluoromethyl)phenyl)propan-1-one (**5a**). Yield: 25%. Mp:
412 69.0-69.5 °C. IR (KBr) ν cm⁻¹: 1683 (s, $\nu_{C=O}$), 1325 (s, ν_{C-F}), 1211 (s, ν_{C-F}), 1164 (s, ν_{C-F}). ¹H
413 NMR (DMSO-*d*₆, 400 MHz) δ ppm: 8.16 (d, 2H, H₂+H₆, $J_{2-3} = J_{6-5} = 8.1$ Hz); 7.90 (d, 2H,
414 H₃+H₅, $J_{3-2} = J_{5-6} = 8.3$ Hz); 7.67 (s, 1H, H₂); 7.22 (s, 1H, H₅); 6.87 (s, 1H, H₄); 4.34 (t, 2H,
415 CH₂-N, $J_{CH_2-CH_2} = 6.8$ Hz); 3.67 (t, 2H, CH₂-CO, $J_{CH_2-CH_2} = 6.8$ Hz). ¹³C NMR (DMSO-*d*₆, 100
416 MHz) δ ppm: 197.27 (CO); 139.32 (C₁); 137.45 (C₂); 132.76 (q, C₄, $^2J = 32.1$ Hz); 128.80 (2C,
417 C₂+C₆), 128.31 (C₄); 125.75 (2C, q, C₃+C₅, $^3J = 3.6$ Hz); 123.75 (q, CF₃ $^1J = 272.8$ Hz); 119.43
418 (C₅); 41.02 (CH₂-N); 39.69 (CH₂-CO). Anal. Calc. for C₁₃H₁₁F₃N₂O: C 58.21%, H 4.13%, N
419 10.44%. Found: C 58.60%, H 4.46%, N 10.46%.

420 3-(1*H*-imidazol-1-yl)-1-(*p*-tolyl)propan-1-one (**6a**). Yield: 24%. Mp: 55.0-56.0 °C. IR
421 (KBr) ν cm⁻¹: 1681 (s, $\nu_{C=O}$). ¹H NMR (DMSO-*d*₆, 400 MHz) δ ppm: 7.87 (d, 2H, H₂+H₆, $J_{2-3} =$
422 $J_{6-5} = 8.2$ Hz); 7.65 (s, 1H, H₂); 7.33 (d, 2H, H₃+H₅, $J_{3-2} = J_{5-6} = 8.0$ Hz); 7.20 (s, 1H, H₅); 6.86
423 (s, 1H, H₄); 4.31 (t, 2H, CH₂-N, $J_{CH_2-CH_2} = 6.8$ Hz); 3.55 (t, 2H, CH₂-CO, $J_{CH_2-CH_2} = 6.8$ Hz);
424 2.37 (s, 3H, CH₃). ¹³C NMR (DMSO-*d*₆, 100 MHz) δ ppm: 197.18 (CO); 143.87 (C₄); 137.41
425 (C₂); 133.80 (C₁); 129.27 (2C, C₃+C₅); 128.23 (C₄); 128.05 (2C, C₂+C₆); 119.41 (C₅); 41.22
426 (CH₂-N); 39.14 (CH₂-CO); 21.13 (CH₃). Anal. Calc. for C₁₃H₁₄N₂O: C 72.87%, H 6.59%, N
427 13.07%. Found: C 72.72%, H 6.68%, N 13.24%.

428 3-(1*H*-imidazol-1-yl)-1-(4-nitrophenyl)propan-1-one (**7a**). Yield: 42%. Mp: 123.0-
429 124.0 °C. IR (KBr) ν cm⁻¹: 1682 (s, $\nu_{C=O}$), 1520 (s, ν_{NO_2}), 1350 (s, ν_{NO_2}). ¹H NMR (DMSO-*d*₆,
430 400 MHz) δ ppm: 8.34 (d, 2H, H₃+H₅, $J_{3-2} = J_{5-6} = 8.8$ Hz); 8.20 (d, 2H, H₂+H₆, $J_{2-3} = J_{6-5} = 8.8$
431 Hz); 7.67 (s, 1H, H₂); 7.21 (s, 1H, H₅); 6.87 (s, 1H, H₄); 4.34 (t, 2H, CH₂-N, $J_{CH_2-CH_2} = 6.8$ Hz);
432 3.69 (t, 2H, CH₂-CO, $J_{CH_2-CH_2} = 6.8$ Hz). ¹³C NMR (DMSO-*d*₆, 100 MHz) δ ppm: 197.02 (CO);
433 150.07 (C₄); 140.71 (C₁); 137.43 (C₂); 129.40 (2C, C₂+C₆); 128.31 (C₄); 123.85 (2C, C₃+C₅);
434 119.41 (C₅); 40.98 (CH₂-N); 39.65 (CH₂-CO). Anal. Calc. for C₁₂H₁₁N₃O₃: C 58.77%, H
435 4.52%, N 17.13%. Found: C 58.74 %, H % 4.71, N % 16.75.

436 3-(1*H*-imidazol-1-yl)-1-(thiophen-3-yl)propan-1-one (**8a**). Yield: 45%. Mp: 86.5-87.0
437 °C. IR (KBr) ν cm⁻¹: 1659 (s, $\nu_{C=O}$). ¹H NMR (DMSO-*d*₆, 400 MHz) δ ppm: 8.53 (dd, 1H, H₂,
438 $J_{2-5} = 2.8$ Hz, $J_{2-4} = 1.3$ Hz); 7.64 (s, 1H, H₂); 7.63 (dd, 1H, H₅, $J_{5-4} = 5.1$ Hz, $J_{5-2} = 2.8$ Hz); 7.51
439 (dd, 1H, H₄, $J_{4-5} = 5.1$ Hz, $J_{4-2} = 1.3$ Hz); 7.19 (s, 1H, H₅); 6.86 (s, 1H, H₄); 4.30 (t, 2H, CH₂-N,
440 $J_{CH_2-CH_2} = 6.8$ Hz); 3.48 (t, 2H, CH₂-CO, $J_{CH_2-CH_2} = 6.8$ Hz). ¹³C NMR (DMSO-*d*₆, 100 MHz) δ
441 ppm: 192.01 (CO); 141.52 (C₃); 137.14 (C₂); 134.12 (C₂); 128.27 (C₄); 127.59 (C₅); 126.37
442 (C₄); 119.40 (C₅); 41.07 (CH₂-N); 40.31 (CH₂-CO). Anal. Calc. for C₁₀H₁₀N₂OS: C 58.23%, H
443 4.89%, N 13.58%. Found: C 57.93%, H 4.97%, N 13.64%.

444 *3-(1H-imidazol-1-yl)-1-(thiophen-2-yl)propan-1-one (9a)*. Yield: 45%. Mp: 75.5-76.0
445 °C. IR (KBr) ν cm^{-1} : 1673 (s, $\nu_{\text{C=O}}$). ^1H NMR (DMSO- d_6 , 400 MHz) δ ppm: 8.02 (dd, 1H, H_5 ,
446 $J_{5,4} = 4.9$ Hz, $J_{5,3} = 1.1$ Hz); 7.98 (dd, 1H, H_3 , $J_{3,4} = 3.8$ Hz, $J_{3,5} = 1.1$ Hz); 7.64 (s, 1H, H_2); 7.24
447 (dd, 1H, H_4 , $J_{4,5} = 4.9$ Hz, $J_{4,3} = 3.8$ Hz); 7.19 (s, 1H, H_5); 6.85 (s, 1H, H_4); 4.31 (t, 2H, $\text{CH}_2\text{-N}$,
448 $J_{\text{CH}_2\text{-CH}_2} = 6.8$ Hz); 3.52 (t, 2H, $\text{CH}_2\text{-CO}$, $J_{\text{CH}_2\text{-CH}_2} = 6.8$ Hz). ^{13}C NMR (DMSO- d_6 , 100 MHz) δ
449 ppm: 190.65 (CO); 143.30 (C_2); 137.40 (C_2'); 135.20 (C_5); 133.80 (C_3); 128.78 (C_4); 128.29
450 (C_4'); 119.39 (C_5'); 41.16 ($\text{CH}_2\text{-N}$); 39.61 ($\text{CH}_2\text{-CO}$). Anal. Calc. for $\text{C}_{10}\text{H}_{10}\text{N}_2\text{OS}$: C 58.23%, H
451 4.89%, N 13.58%. Found: C 58.04%, H 5.07%, N 14.07%.

452 *1-(furan-2-yl)-3-(1H-imidazol-1-yl)propan-1-one (10a)*. Yield: 21%. Mp: 92.0-93.0 °C.
453 IR (KBr) ν cm^{-1} : 1684 (s, $\nu_{\text{C=O}}$). ^1H NMR (DMSO- d_6 , 400 MHz) δ ppm: 7.99 (dd, 1H, H_5 , $J_{5,4} =$
454 1.6 Hz, $J_{5,3} = 0.6$ Hz); 7.62 (s, 1H, H_2); 7.50 (dd, 1H, H_3 , $J_{3,4} = 3.6$ Hz, $J_{3,5} = 0.5$ Hz); 7.17 (s,
455 1H, H_5); 6.85 (s, 1H, H_4); 6.71 (dd, 1H, H_4 , $J_{4,3} = 3.6$ Hz, $J_{4,5} = 1.7$ Hz); 4.30 (t, 2H, $\text{CH}_2\text{-N}$,
456 $J_{\text{CH}_2\text{-CH}_2} = 6.8$ Hz); 3.37 (t, 2H, $\text{CH}_2\text{-CO}$, $J_{\text{CH}_2\text{-CH}_2} = 6.8$ Hz). ^{13}C NMR (DMSO- d_6 , 100 MHz) δ
457 ppm: 185.78 (CO); 151.57 (C_2); 148.04 (C_5); 137.39 (C_2'); 128.31 (C_4); 119.35 (C_5'); 119.03
458 (C_3); 112.55 (C_4); 40.89 ($\text{CH}_2\text{-N}$); 38.96 ($\text{CH}_2\text{-CO}$). Anal. Calc. for $\text{C}_{10}\text{H}_{10}\text{N}_2\text{O}_2$: C 63.15%, H
459 5.30%, N 14.73%. Found: C 63.35%, H 5.29%, N 15.11%.

460 *3-(1H-imidazol-1-yl)-1-(naphthalene-2-yl)propan-1-one (11a)*. Yield: 24%. Mp: 110.5-
461 111.5 °C. IR (KBr) ν cm^{-1} : 1682 (s, $\nu_{\text{C=O}}$). ^1H NMR (DMSO- d_6 , 400 MHz) δ ppm: 8.70 (s, 1H,
462 H_1); 8.12 (d, 1H, H_3 , $J_{3,4} = 7.9$ Hz); 8.03-7.97 (m, 3H, $\text{H}_4 + \text{H}_6 + \text{H}_9$); 7.71 (s, 1H, H_2); 7.70-
463 7.61 (m, 2H, $\text{H}_8 + \text{H}_7$); 7.25 (s, 1H, H_5); 6.88 (s, 1H, H_4); 4.39 (t, 2H, $\text{CH}_2\text{-N}$, $J_{\text{CH}_2\text{-CH}_2} = 6.9$
464 Hz); 3.74 (t, 2H, $\text{CH}_2\text{-CO}$, $J_{\text{CH}_2\text{-CH}_2} = 6.9$ Hz). ^{13}C NMR (DMSO- d_6 , 100 MHz) δ ppm: 197.62
465 (CO); 137.44 (C_2); 135.14 (C_5); 133.50 (C_{10}); 132.15 (C_2); 130.14 (C_1); 129.60 (C_3); 128.76
466 (C_7); 128.33 (C_4'); 128.21 (C_8); 127.67 (C_9); 126.98 (C_4); 123.31 (C_6); 119.49 (C_5'); 41.35
467 ($\text{CH}_2\text{-N}$); 39.42 ($\text{CH}_2\text{-CO}$). Anal. Calc. for $\text{C}_{16}\text{H}_{14}\text{N}_2\text{O}$: C 76.78%, H 5.64%, N 11.19%. Found:
468 C 76.63%, 5.47H %, N 11.06%.

469 *1-(benzo[b]thiophen-3-yl)-3-(1H-imidazol-1-yl)propan-1-one (12a)*. Yield: 33%. Mp:
470 105.0-106.0 °C. IR (KBr) ν cm^{-1} : 1666 (s, $\nu_{\text{C=O}}$). ^1H NMR (DMSO- d_6 , 400 MHz) δ ppm: 9.00
471 (s, 1H, H_2); 8.61 (dd, 1H, H_5 , $J_{5,6} = 8.0$ Hz, $J_{5,8} = 0.7$ Hz); 8.08 (dd, 1H, H_8 , $J_{8,7} = 7.9$ Hz, $J_{8,5} =$
472 0.5 Hz); 7.68 (s, 1H, H_2'); 7.53-7.44 (m, 2H, $\text{H}_6 + \text{H}_7$); 7.23 (s, 1H, H_5); 6.87 (s, 1H, H_4); 4.37 (t,
473 2H, $\text{CH}_2\text{-N}$, $J_{\text{CH}_2\text{-CH}_2} = 6.8$ Hz); 3.62 (t, 2H, $\text{CH}_2\text{-CO}$, $J_{\text{CH}_2\text{-CH}_2} = 6.9$ Hz). ^{13}C NMR (DMSO- d_6 ,
474 100 MHz) δ ppm: 193.12 (CO); 140.21 (C_2); 139.35 (C_3); 137.42 (C_2'); 136.07 (C_4); 133.82
475 (C_9); 128.29 (C_4'); 125.82 (C_6); 125.40 (C_7); 124.61 (C_5); 122.91 (C_8); 119.43 (C_5'); 41.25
476 ($\text{CH}_2\text{-N}$); 40.67 ($\text{CH}_2\text{-CO}$). Anal. Calc. for $\text{C}_{14}\text{H}_{12}\text{N}_2\text{OS}$: C 65.60%, H 4.72%, N 10.93%.
477 Found: C 65.75%, H 5.03%, N 10.86%.

478 *1-(benzo[b]thiophen-2-yl)-3-(1H-imidazol-1-yl)propan-1-one (13a)*. Yield: 31%. Mp:
479 149.0-150.0 °C. IR (KBr) ν cm^{-1} : 1660 (s, $\nu_{\text{C=O}}$). ^1H NMR (DMSO- d_6 , 400 MHz) δ ppm: 8.40
480 (s, 1H, H_3); 8.05 (d, 1H, H_8 , $J_{8,7} = 8.1$ Hz); 8.01 (d, 1H, H_5 , $J_{5,6} = 7.8$ Hz); 7.67 (s, 1H, H_2); 7.54

481 (t, 1H, **H**₆, $J_{6.5} = J_{6.7} = 7.1$ Hz); 7.47 (t, 1H, **H**₇, $J_{7.8} = J_{7.6} = 7.2$ Hz); 7.23 (s, 1H, **H**₅); 6.87 (s, 1H,
482 **H**₄); 4.36 (t, 2H, **CH**₂-**N**, $J_{CH_2-CH_2} = 6.8$ Hz); 3.66 (t, 2H, **CH**₂-**CO**, $J_{CH_2-CH_2} = 6.8$ Hz). ¹³C NMR
483 (DMSO-*d*₆, 100 MHz) δ ppm: 192.42 (**CO**); 142.58 (**C**₉); 141.52 (**C**₄); 139.04 (**C**₂); 137.42
484 (**C**₂); 131.26 (**C**₃); 128.33 (**C**₄); 127.84 (**C**₆); 126.35 (**C**₅); 125.30 (**C**₇); 123.15 (**C**₈); 119.39
485 (**C**₅); 41.18 (**CH**₂-**N**); 39.61 (**CH**₂-**CO**). Anal. Calc. for C₁₄H₁₂N₂OS: C 65.60%, H 4.72%, N
486 10.93%. Found: C 65.66%, H 5.07%, N 10.74%.

487 *1*-(benzofuran-2-yl)-3-(1*H*-imidazol-1-yl)propan-1-one (**14a**). Yield: 26%. Mp: 131.0-
488 132.0 °C. IR (KBr) ν cm⁻¹: 1677 (s, ν_{C=O}). ¹H NMR (DMSO-*d*₆, 400 MHz) δ ppm: 7.95 (d, 1H,
489 **H**₃, $J_{3.5} = 0.7$ Hz); 7.83 (d, 1H, **H**₅, $J_{5.6} = 7.8$ Hz); 7.71 (dd, 1H, **H**₈, $J_{8.7} = 8.4$ Hz, $J_{8.6} = 0.6$ Hz);
490 7.66 (s, 1H, **H**₂); 7.54 (td, 1H, **H**₇, $J_{7.8} = 8.4$ Hz, $J_{7.6} = 7.3$ Hz, $J_{7.5} = 1.2$ Hz); 7.37 (t, 1H, **H**₆, $J_{6.5}$
491 $= J_{6.7} = 7.9$ Hz); 7.21 (s, 1H, **H**₅); 6.86 (s, 1H, **H**₄); 4.36 (t, 2H, **CH**₂-**N**, $J_{CH_2-CH_2} = 6.8$ Hz); 3.54
492 (t, 2H, **CH**₂-**CO**, $J_{CH_2-CH_2} = 6.8$ Hz). ¹³C NMR (DMSO-*d*₆, 100 MHz) δ ppm: 187.97 (**CO**);
493 155.00 (**C**₉); 151.62 (**C**₂); 137.43 (**C**₂); 128.67 (**C**₇); 128.35 (**C**₄); 126.68 (**C**₄); 124.11 (**C**₆);
494 123.75 (**C**₅); 119.39 (**C**₅); 114.59 (**C**₃); 112.26 (**C**₈); 40.91 (**CH**₂-**N**); 39.46 (**CH**₂-**CO**). Anal.
495 Calc. for C₁₄H₁₂N₂O₂: C 69.99%, H 5.03%, N 11.66%. Found: C 70.35%, H 5.25%, N 11.63%.

496 *1*-(4-bromophenyl)-3-(1*H*-imidazol-1-yl)propan-1-one (**15a**). Yield: 23%. Mp: 95.5-
497 96.5 °C. IR (KBr) ν cm⁻¹: 1686 (s, ν_{C=O}). ¹H NMR (DMSO-*d*₆, 400 MHz) δ ppm: 7.91 (d, 2H,
498 **H**₂+**H**₆, $J_{2.3} = J_{6.5} = 8.6$ Hz); 7.74 (d, 2H, **H**₃+**H**₅, $J_{3.2} = J_{5.6} = 8.6$ Hz); 7.66 (s, 1H, **H**₂); 7.21 (s,
499 1H, **H**₅); 6.86 (s, 1H, **H**₄); 4.32 (t, 2H, **CH**₂-**N**, $J_{CH_2-CH_2} = 6.8$ Hz); 3.59 (t, 2H, **CH**₂-**CO**, $J_{CH_2-CH_2}$
500 $= 6.8$ Hz). ¹³C NMR (DMSO-*d*₆, 100 MHz) δ ppm: 196.98 (**CO**); 137.43 (**C**₂); 135.19 (**C**₁);
501 131.81 (2C, **C**₃+**C**₅); 129.98 (2C, **C**₂+**C**₆); 128.27 (**C**₄); 127.61 (**C**₄); 119.42 (**C**₅); 41.08 (**CH**₂-
502 **N**); 39.31 (**CH**₂-**CO**). Anal. Calc. for C₁₂H₁₁BrN₂O: C 51.63%, H 3.97%, N 10.04%. Found: C
503 52.01%, H 4.01%, N 10.03%.

504 *3*-(1*H*-imidazol-1-yl)-1-(4-(trifluoromethoxy)phenyl)propan-1-one (**16a**). Yield: 23%.
505 Mp: 45.0-46.0 °C. IR (KBr) ν cm⁻¹: 1691 (s, ν_{C=O}), 1265 (s, ν_{C-F}), 1213 (s, ν_{C-F}), 1161 (s, ν_{C-F}).
506 ¹H NMR (DMSO-*d*₆, 400 MHz) δ ppm: 8.11 (d, 2H, **H**₂+**H**₆, $J_{2.3} = J_{6.5} = 8.9$ Hz); 7.66 (s, 1H,
507 **H**₂); 7.51 (d, 2H, **H**₃+**H**₅, $J_{3.2} = J_{5.6} = 8.0$ Hz); 7.20 (s, 1H, **H**₅); 6.86 (s, 1H, **H**₄); 4.32 (t, 2H,
508 **CH**₂-**N**, $J_{CH_2-CH_2} = 6.8$ Hz); 3.62 (t, 2H, **CH**₂-**CO**, $J_{CH_2-CH_2} = 6.8$ Hz). ¹³C NMR (DMSO-*d*₆, 100
509 MHz) δ ppm: 196.57 (**CO**); 151.72 (**C**₄); 137.45 (**C**₂); 135.07 (**C**₁); 130.52 (2C, **C**₂+**C**₆); 128.29
510 (**C**₄); 120.80 (2C, **C**₃+**C**₅); 119.93 (q, **CF**₃, $^1J = 262.7$ Hz); 119.43 (**C**₅); 41.07 (**CH**₂-**N**); 39.40
511 (**CH**₂-**CO**). Anal. Calc. for C₁₃H₁₁F₃N₂O₂: C 54.93%, H 3.90%, N 9.86%. Found: C 54.8%, H
512 3.85%, N 9.9%.

513 *4*-(3-(1*H*-imidazol-1-yl)propanoyl)benzotrile (**17a**). Yield: 30%. Mp: 110.0-111.0 °C.
514 IR (KBr) ν cm⁻¹: 2230 (s, ν_{C≡N}), 1685 (s, ν_{C=O}). ¹H NMR (DMSO-*d*₆, 400 MHz) δ ppm: 8.11 (d,
515 2H, **H**₂+**H**₆, $J_{2.3} = J_{6.5} = 8.6$ Hz); 8.01 (d, 2H, **H**₃+**H**₅, $J_{3.2} = J_{5.6} = 8.5$ Hz); 7.66 (s, 1H, **H**₂); 7.20
516 (s, 1H, **H**₅); 6.86 (s, 1H, **H**₄); 4.33 (t, 2H, **CH**₂-**N**, $J_{CH_2-CH_2} = 6.8$ Hz); 3.66 (t, 2H, **CH**₂-**CO**, J_{CH_2-

517 $\text{CH}_2 = 6.8 \text{ Hz}$). ^{13}C NMR (DMSO- d_6 , 100 MHz) δ ppm: 197.23 (CO); 139.28 (C₁); 137.43 (C_{2'});
518 132.81 (2C, C₃+C₅); 128.58 (2C, C₂+C₆); 128.29 (C_{4'}); 119.41 (C_{5'}); 118.10 (CN); 115.39 (C₄);
519 40.98 (CH₂-N); 39.64 (CH₂-CO). Anal. Calc. for C₁₃H₁₁N₃O: C 69.32%, H 4.92%, N 18.66%.
520 Found: C 69.98%, H 5.13%, N 18.31%.

521 *3-(1H-imidazol-1-yl)-1-(o-tolyl)propan-1-one (18a)*. Yield: 30%. Mp: 53.5-54.5 °C. IR
522 (KBr) $\nu \text{ cm}^{-1}$: 1668 (s, $\nu_{\text{C=O}}$). ^1H NMR (DMSO- d_6 , 400 MHz) δ ppm: 7.77 (d, 1H, H₆, $J_{6,5} = 7.7$
523 Hz); 7.65 (s, 1H, H_{2'}); 7.44 (t, 1H, H₄, $J_{4,3} = J_{4,5} = 7.5 \text{ Hz}$); 7.44 (m, 2H, H₃+H₅, $J_{3,4} = J_{5,4} = 7.5$
524 Hz); 7.20 (s, 1H, H_{5'}); 6.87 (s, 1H, H_{4'}); 4.31 (t, 2H, CH₂-N, $J_{\text{CH}_2\text{-CH}_2} = 6.7 \text{ Hz}$); 3.50 (t, 2H,
525 CH₂-CO, $J_{\text{CH}_2\text{-CH}_2} = 6.7 \text{ Hz}$); 2.36 (s, 3H, CH₃). ^{13}C NMR (DMSO- d_6 , 100 MHz) δ ppm: 201.51
526 (CO); 137.42 (C_{2'}); 137.20 (C₁); 137.13 (C₂); 131.66 (C₃); 131.57 (C₄); 128.79 (C₆); 128.28
527 (C_{4'}); 125.93 (C₅); 119.35 (C_{5'}); 41.93 (CH₂-N); 41.34 (CH₂-CO); 20.64 (CH₃). Anal. Calc. for
528 C₁₃H₁₄N₂O: C 72.87%, H 6.59%, N 13.07%. Found: C 72.96%, H 6.37%, N 12.94%.

529 *3-(1H-imidazol-1-yl)-1-(3-nitrophenyl)propan-1-one (19a)*. Yield: 44%. Mp: 83.5-84.5
530 °C. IR (KBr) $\nu \text{ cm}^{-1}$: 1686 (s, $\nu_{\text{C=O}}$), 1526 (s, ν_{NO_2}), 1359 (s, ν_{NO_2}). ^1H NMR (DMSO- d_6 , 400
531 MHz) δ ppm: 8.66 (s, 1H, H₂); 8.47 (d, 1H, H₄, $J_{4,5} = 8.2 \text{ Hz}$, $J_{4,2} = J_{4,6} = 1.4 \text{ Hz}$); 8.39 (d, 1H,
532 H₆, $J_{6,5} = 7.8 \text{ Hz}$); 7.83 (t, 1H, H₅, $J_{5,4} = J_{5,6} = 8.0 \text{ Hz}$); 7.68 (s, 1H, H_{2'}); 7.22 (s, 1H, H_{5'}); 6.87 (s,
533 1H, H_{4'}); 4.36 (t, 2H, CH₂-N, $J_{\text{CH}_2\text{-CH}_2} = 6.7 \text{ Hz}$); 3.73 (t, 2H, CH₂-CO, $J_{\text{CH}_2\text{-CH}_2} = 6.7 \text{ Hz}$). ^{13}C
534 NMR (DMSO- d_6 , 100 MHz) δ ppm: 196.83 (CO); 148.53 (C₃); 137.93 (C_{2'}); 137.80 (C₁);
535 134.64 (C₆); 131.09 (C₅); 128.74 (C_{4'}); 128.11 (C₄); 122.81 (C₂); 119.93 (C_{5'}); 41.44 (CH₂-N);
536 40.07 (CH₂-CO). Anal. Calc. for C₁₂H₁₁N₃O₃: C 58.77%, H 4.52%, N 17.13%. Found: C
537 58.49%, H 4.61%, N 16.98%.

538 *1-(3,4-difluorophenyl)-3-(1H-imidazol-1-yl)propan-1-one (20a)*. Yield: 24%. Mp: 95.5-
539 96.5 °C. IR (KBr) $\nu \text{ cm}^{-1}$: 1682 (s, $\nu_{\text{C=O}}$), 1284 (s, $\nu_{\text{C-F}}$). ^1H NMR (DMSO- d_6 , 400 MHz) δ ppm:
540 8.02 (ddd, 1H, H₂, $J_{2-F} = 11.3 \text{ Hz}$, $J_{2-F'} = 7.9 \text{ Hz}$, $J_{2,6} = 2.1 \text{ Hz}$); 7.86-7.90 (m, 1H, H₆); 7.65 (s,
541 1H, H_{2'}); 7.60 (dt, 1H, H₅, $J_{5-F} = 10.4 \text{ Hz}$, $J_{5-F'} = J_{5,6} = 8.4 \text{ Hz}$); 7.20 (s, 1H, H_{5'}); 6.86 (s, 1H,
542 H_{4'}); 4.31 (t, 2H, CH₂-N, $J_{\text{CH}_2\text{-CH}_2} = 6.8 \text{ Hz}$); 3.60 (t, 2H, CH₂-CO, $J_{\text{CH}_2\text{-CH}_2} = 6.8 \text{ Hz}$). ^{13}C NMR
543 (DMSO- d_6 , 100 MHz) δ ppm: 195.67 (CO); 152.75 (dd, C₃, $^1J = 253.8 \text{ Hz}$, $^2J = 12.8 \text{ Hz}$);
544 149.47 (dd, C₄, $^1J = 247.9 \text{ Hz}$, $^2J = 13.1 \text{ Hz}$); 137.41 (C_{2'}); 133.72 (C₁); 128.27 (C_{4'}); 125.82
545 (dd, C₆, $^3J = 7.9 \text{ Hz}$, $^4J = 3.5 \text{ Hz}$); 119.40 (C_{5'}); 117.98 (d, C₅, $^2J = 17.9 \text{ Hz}$); 117.35 (d, C₂, $^2J =$
546 18.1 Hz); 41.04 (CH₂-N); 39.31 (CH₂-CO). Anal. Calc. for C₁₂H₁₀F₂N₂O: C 61.02%, H 4.27%,
547 N 11.86%. Found: C 61.31%, H 4.4%, N 11.84%.

548 *1-(4-chloro-3-fluorophenyl)-3-(1H-imidazol-1-yl)propan-1-one (21a)*. Yield: 21%. Mp:
549 110.0-111.0 °C. IR (KBr) $\nu \text{ cm}^{-1}$: 1682 (s, $\nu_{\text{C=O}}$), 1229 (s, $\nu_{\text{C-F}}$). ^1H NMR (DMSO- d_6 , 400 MHz)
550 δ ppm: 7.96 (dd, 1H, H₂, $J_{2-F} = 10.1 \text{ Hz}$, $J_{2,6} = 1.9 \text{ Hz}$); 7.83 (dd, 1H, H₆, $J_{6,5} = 8.5 \text{ Hz}$, $J_{6,2} = 1.8$
551 Hz); 7.77 (dd, 1H, H₅, $J_{5,6} = 7.2 \text{ Hz}$, $J_{5-F} = 5.5 \text{ Hz}$); 7.65 (s, 1H, H_{2'}); 7.20 (s, 1H, H_{5'}); 6.86 (s,
552 1H, H_{4'}); 4.32 (t, 2H, CH₂-N, $J_{\text{CH}_2\text{-CH}_2} = 6.8 \text{ Hz}$); 3.61 (t, 2H, CH₂-CO, $J_{\text{CH}_2\text{-CH}_2} = 6.8 \text{ Hz}$). ^{13}C
553 NMR (DMSO- d_6 , 100 MHz) δ ppm: 196.01 (d, CO, $^4J = 1.8 \text{ Hz}$); 157.25 (d, C₃, $^1J = 248.2 \text{ Hz}$);

554 137.41 (**C**₂); 136.89 (d, **C**₁, ³*J* = 5.6 Hz); 131.17 (**C**₅); 128.28 (**C**₄); 125.17 (d, **C**₆, ⁴*J* = 3.6 Hz);
555 124.99 (d, **C**₄, ²*J* = 17.6 Hz); 119.40 (**C**₅); 116.12 (d, **C**₂, ²*J* = 21.9 Hz); 41.00 (**CH**₂-**N**); 39.42
556 (**CH**₂-**CO**). Anal. Calc. for C₁₂H₁₀ClFN₂O: C 57.04%, H 3.99%, N 11.09%. Found: C 57.18%,
557 H 4.05%, N 11.16%.

558 *1-(3-chloro-4-fluorophenyl)-3-(1H-imidazol-1-yl)propan-1-one (22a)*. Yield: 26%. Mp:
559 94.0-95.0 °C. IR (KBr) ν cm⁻¹: 1687 (s, $\nu_{C=O}$), 1248 (s, ν_{C-F}). ¹H NMR (DMSO-*d*₆, 400 MHz) δ
560 ppm: 8.18 (dd, 1H, **H**₂, *J*_{2-F} = 7.2 Hz, *J*₂₋₆ = 2.2 Hz); 8.00 (ddd, 1H, **H**₆, *J*₆₋₅ = 8.6 Hz, *J*_{6-F} = 4.8
561 Hz, *J*₆₋₂ = 2.2 Hz); 7.65 (s, 1H, **H**₂); 7.58 (t, 1H, **H**₅, *J*_{5-F} = *J*₅₋₆ = 8.9 Hz); 7.20 (s, 1H, **H**₅); 6.86
562 (s, 1H, **H**₄); 4.31 (t, 2H, **CH**₂-**N**, *J*_{CH₂-CH₂} = 6.8 Hz); 3.62 (t, 2H, **CH**₂-**CO**, *J*_{CH₂-CH₂} = 6.8 Hz). ¹³C
563 NMR (DMSO-*d*₆, 100 MHz) δ ppm: 195.64 (**CO**); 160.19 (d, **C**₄, ¹*J* = 254.0 Hz); 137.41 (**C**₂);
564 133.94 (d, **C**₁, ⁴*J* = 3.5 Hz); 130.75 (**C**₂); 129.30 (d, **C**₆, ³*J* = 8.8 Hz); 128.25 (**C**₄); 120.30 (d, **C**₃,
565 ²*J* = 18.2 Hz); 119.41 (**C**₅); 117.36 (d, **C**₅, ²*J* = 21.5 Hz); 41.03 (**CH**₂-**N**); 39.28 (**CH**₂-**CO**).
566 Anal. Calc. for C₁₂H₁₀ClFN₂O: C 57.04%, H 3.99%, N 11.09%. Found: C 56.87%, H 4.14%, N
567 11.14%.

568 *1-(3-bromo-4-fluorophenyl)-3-(1H-imidazol-1-yl)propan-1-one (23a)*. Yield: 26%. Mp:
569 118.5-119.5 °C. IR (KBr) ν cm⁻¹: 1686 (s, $\nu_{C=O}$), 1245 (s, ν_{C-F}). ¹H NMR (DMSO-*d*₆, 400 MHz)
570 δ ppm: 8.29 (dd, 1H, **H**₂, *J*_{2-F} = 6.7 Hz, *J*₂₋₆ = 2.1 Hz); 8.03 (ddd, 1H, **H**₆, *J*₆₋₅ = 8.6 Hz, *J*_{6-F} = 4.9
571 Hz, *J*₆₋₂ = 2.2 Hz); 7.65 (s, 1H, **H**₂); 7.53 (t, 1H, **H**₅, *J*_{5-F} = *J*₅₋₆ = 8.6 Hz); 7.20 (s, 1H, **H**₅); 6.86
572 (s, 1H, **H**₄); 4.31 (t, 2H, **CH**₂-**N**, *J*_{CH₂-CH₂} = 6.8 Hz); 3.62 (t, 2H, **CH**₂-**CO**, *J*_{CH₂-CH₂} = 6.8 Hz). ¹³C
573 NMR (DMSO-*d*₆, 100 MHz) δ ppm: 195.56 (**CO**); 161.24 (d, **C**₄, ¹*J* = 252.3 Hz); 137.41 (**C**₂);
574 134.24 (d, **C**₁, ⁴*J* = 3.4 Hz); 133.63 (d, **C**₂, ³*J* = 1.2 Hz); 129.95 (d, **C**₆, ³*J* = 8.9 Hz); 128.25
575 (**C**₄); 119.41 (**C**₅); 117.14 (d, **C**₅, ²*J* = 22.8 Hz); 108.74 (d, **C**₃, ²*J* = 21.7 Hz); 41.03 (**CH**₂-**N**);
576 39.26 (**CH**₂-**CO**). Anal. Calc. for C₁₂H₁₀BrFN₂O: C 48.51%, H 3.39%, N 9.43%. Found: C
577 48.84%, H 3.70%, N 9.49%.

578 *1-(3,4-dimethoxyphenyl)3-(1H-imidazol-1-yl)propan-1-one (24a)*. Yield: 23%. Mp:
579 149.0-150.0 °C. IR (KBr) ν cm⁻¹: 1671 (s, $\nu_{C=O}$). ¹H NMR (DMSO-*d*₆, 400 MHz) δ ppm: 7.64
580 (m, 2H, **H**₂+**H**₂); 7.45 (d, 1H, **H**₆, *J*₆₋₂ = 2.0 Hz); 7.20 (s, 1H, **H**₅); 7.06 (d, 2H, **H**₅, *J*₅₋₆ = 8.5
581 Hz); 6.85 (s, 1H, **H**₄); 4.31 (t, 2H, **CH**₂-**N**, *J*_{CH₂-CH₂} = 6.8 Hz); 3.84 (s, 3H, **OCH**₃); 3.81 (s, 3H,
582 **OCH**₃); 3.53 (t, 2H, **CH**₂-**CO**, *J*_{CH₂-CH₂} = 6.8 Hz). ¹³C NMR (DMSO-*d*₆, 100 MHz) δ ppm:
583 196.07 (**CO**); 153.29 (**C**₄); 148.58 (**C**₃); 137.45 (**C**₂); 129.21 (**C**₁); 128.22 (**C**₄); 122.74 (**C**₂);
584 119.47 (**C**₅); 110.89 (**C**₅); 110.16 (**C**₆); 55.76 (**C**₂); 55.52 (**C**₁); 41.38 (**CH**₂-**N**); 38.84 (**CH**₂-
585 **CO**). Anal. Calc. for C₁₄H₁₆N₂O₃: C 64.60%, H 6.20%, N 10.76%. Found: C 64.33%, H 6.33%,
586 N 10.74%.

587 *1-(2,4-dimethoxyphenyl)3-(1H-imidazol-1-yl)propan-1-one (25a)*. Yield: 25%. Mp:
588 58.0-59.0 °C. IR (KBr) ν cm⁻¹: 1673 (s, $\nu_{C=O}$). ¹H NMR (DMSO-*d*₆, 400 MHz) δ ppm: 7.67 (d,
589 1H, **H**₆, *J*₆₋₅ = 8.7 Hz), 7.61 (s, 1H, **H**₂); 7.15 (s, 1H, **H**₅); 6.84 (s, 1H, **H**₄); 6.65-6.60 (m, 2H,
590 **H**₅+**H**₃); 4.27 (t, 2H, **CH**₂-**N**, *J*_{CH₂-CH₂} = 6.8 Hz); 3.87 (s, 3H, **OCH**₃); 3.83 (s, 3H, **OCH**₃); 3.38

591 (t, 2H, **CH₂-CO**, $J_{CH_2-CH_2} = 6.8$ Hz). ¹³C NMR (DMSO-*d*₆, 100 MHz) δ ppm: 196.19 (**CO**);
592 164.57 (**C₄**); 160.97 (**C₂**); 137.40 (**C_{2'}**); 131.91 (**C₆**); 128.21 (**C_{4'}**); 119.59 (**C_{5'}**); 119.43 (**C₁**);
593 106.16 (**C₃**); 98.45 (**C₃**); 55.91 (**OCH₃**); 55.65 (**OCH₃**); 44.42 (**CH₂-N**); 41.49 (**CH₂-CO**). Anal.
594 Calc. for C₁₄H₁₆N₂O₃: C 64.60%, H 6.20%, N 10.76%. Found: C 64.78%, H 6.02%, N 10.61%.

595 *1-(3,5-dimethoxyphenyl)-3-(1H-imidazol-1-yl)propan-1-one (26a)*. Yield: 32%. Mp:
596 93.0-94.0 °C. IR (KBr) ν cm⁻¹: 1675 (s, ν_{C=O}). ¹H NMR (DMSO-*d*₆, 400 MHz) δ ppm: 7.65 (s,
597 1H, **H_{2'}**); 7.20 (s, 1H, **H_{5'}**); 7.08 (d, 2H, **H₂+H₆**, $J_{2-4} = J_{6-4} = 2.3$ Hz); 6.86 (s, 1H, **H_{4'}**); 6.77 (t,
598 1H, **H₄**, $J_{4-2} = J_{2-6} = 2.3$ Hz); 4.31 (t, 2H, **CH₂-N**, $J_{CH_2-CH_2} = 6.7$ Hz); 3.80 (s, 6H, **OCH₃**); 3.58 (t,
599 2H, **CH₂-CO**, $J_{CH_2-CH_2} = 6.8$ Hz). ¹³C NMR (DMSO-*d*₆, 100 MHz) δ ppm: 197.40 (**CO**); 160.59
600 (2C, **C₃+C₅**); 138.27 (**C₁**); 137.44 (**C_{2'}**); 128.21 (**C_{4'}**); 119.45 (**C_{5'}**); 105.69 (2C, **C₂+C₆**); 105.35
601 (**C₄**); 55.52 (2C, **C₁+C₂**); 41.19 (**CH₂-N**); 39.39 (**CH₂-CO**). Anal. Calc. for C₁₄H₁₆N₂O₃: C
602 64.60%, H 6.20%, N 10.76%. Found: C 64.33%, H 6.33%, N 10.74%.

603 *3-(1H-imidazol-1-yl)-1-(3,4,5-trimethoxyphenyl)propan-1-one (27a)*. Yield: 38%. Mp:
604 122.0-123.0 °C. IR (KBr) ν cm⁻¹: 1669 (s, ν_{C=O}). ¹H NMR (DMSO-*d*₆, 400 MHz) δ ppm: 7.67
605 (s, 1H, **H_{2'}**); 7.26 (s, 2H, **H₂+H₆**); 7.21 (s, 1H, **H_{5'}**); 6.87 (s, 1H, **H_{4'}**); 4.32 (t, 2H, **CH₂-N**, $J_{CH_2-CH_2}$
606 $= 6.7$ Hz); 3.85 (s, 6H, **OCH₃**); 3.74 (s, 3H, **OCH₃**); 3.59 (t, 2H, **CH₂-CO**, $J_{CH_2-CH_2} = 6.8$ Hz).
607 ¹³C NMR (DMSO-*d*₆, 100 MHz) δ ppm: 196.59 (**CO**); 152.78 (2C, **C₃+C₅**); 142.08 (**C₄**); 137.44
608 (**C_{2'}**); 131.57 (**C₁**); 128.16 (**C_{4'}**); 119.52 (**C_{5'}**); 105.57 (2C, **C₂+C₆**); 60.15 (**C₂**); 56.08 (2C,
609 **C₁+C₃**); 41.33 (**CH₂-N**); 38.88 (**CH₂-CO**). Anal. Calc. for C₁₅H₁₈N₂O₄: C 62.06%, H 6.25%, N
610 9.65%. Found: C 61.94%, H 6.14%, N 9.57%.

611 *1-(4-fluoronaphthalen-1-yl)-3-(1H-imidazol-1-yl)-1-propan-1-one (28a)*. Yield: 22%.
612 Mp: 60.5-61.5 °C. IR (KBr) ν cm⁻¹: 1667 (s, ν_{C=O}), 1233 (s, ν_{C-F}). ¹H NMR (DMSO-*d*₆, 400
613 MHz) δ ppm: 8.62 (d, 1H, **H₉**, $J_{9-8} = 8.1$ Hz); 8.20 (dd, 1H, **H₂**, $J_{2-3} = 8.2$ Hz, $J_{2-F} = 5.6$ Hz); 8.13
614 (d, 1H, **H₆**, $J_{6-7} = 8.8$ Hz); 7.75-7.67 (m, 3H, **H₇ + H₈ + H_{2'}**); 7.44 (dd, 1H, **H₃**, $J_{3-F} = 10.3$ Hz, J_{3-2}
615 $= 8.2$ Hz); 7.24 (s, 1H, **H_{5'}**); 6.88 (s, 1H, **H_{4'}**); 4.39 (t, 2H, **CH₂-N**, $J_{CH_2-CH_2} = 6.7$ Hz); 3.69 (t, 2H,
616 **CH₂-CO**, $J_{CH_2-CH_2} = 6.8$ Hz). ¹³C NMR (DMSO-*d*₆, 100 MHz) δ ppm: 200.27 (**CO**); 160.22 (d,
617 **C₄**, $^1J = 257.7$ Hz); 137.47 (**C_{2'}**); 131.44 (d, **C₁₀**, $^3J = 5.2$ Hz); 130.97 (d, **C₁**, $^4J = 4.2$ Hz);
618 130.29 (d, **C₂**, $^3J = 10.1$ Hz); 129.17 (**C₈**); 128.32 (**C_{4'}**); 127.23 (d, **C₇**, $^4J = 1.2$ Hz); 125.61 (d,
619 **C₉**, $^4J = 2.2$ Hz); 123.12 (d, **C₅**, $^2J = 15.9$ Hz); 120.29 (d, **C₆**, $^3J = 6.2$ Hz); 119.42 (**C_{5'}**); 108.78
620 (d, **C₃**, $^2J = 20.5$ Hz); 42.09 (**CH₂-N**); 41.51 (**CH₂-CO**). Anal. Calc. for C₁₆H₁₃FN₂O: C 71.63%,
621 H 4.88%, N 10.44%. Found: C 71.49%, H 4.72%, N 10.67%.

622 *1-(5-fluorobenzothien-3-yl)-3-(1H-imidazol-1-yl)propan-1-one (29a)*. Yield:
623 18%. Mp: 101.0-102.0 °C. IR (KBr) ν cm⁻¹: 1654 (s, ν_{C=O}), 1185 (s, ν_{C-F}). ¹H NMR (DMSO-*d*₆,
624 400 MHz) δ ppm: 9.10 (s, 1H, **H₂**); 8.29 (dd, 1H, **H₅**, $J_{5-F} = 10.6$ Hz, $J_{5-7} = 2.6$ Hz); 8.14 (dd, 1H,
625 **H₈**, $J_{8-7} = 8.9$ Hz, $J_{8-F} = 5.1$ Hz); 7.68 (s, 1H, **H_{2'}**); 7.37 (td, 1H, **H₇**, $J_{7-F} = J_{7-8} = 8.9$ Hz, $J_{7-5} = 2.6$
626 Hz); 7.22 (s, 1H, **H_{5'}**); 6.86 (s, 1H, **H_{4'}**); 4.36 (t, 2H, **CH₂-N**, $J_{CH_2-CH_2} = 6.8$ Hz); 3.60 (t, 2H,
627 **CH₂-CO**, $J_{CH_2-CH_2} = 6.8$ Hz). ¹³C NMR (DMSO-*d*₆, 100 MHz) δ ppm: 193.16 (**CO**); 161.15 (d,

628 C₆, ¹J = 240.4 Hz); 142.88 (C₂); 137.53 (C_{2'}); 137.40 (d, C₄, ³J = 10.6 Hz); 135.22 (d, C₃, ⁴J =
629 1.0 Hz); 133.40 (d, C₉, ⁴J = 4.6 Hz); 128.33 (C_{4'}); 124.86 (d, C₈, ³J = 9.7 Hz); 119.58 (C_{5'});
630 114.21 (d, C₇, ²J = 25.2 Hz); 110.03 (d, C₅, ²J = 24.9 Hz); 41.28 (CH₂-N); 40.62 (CH₂-CO).
631 Anal. Calc. for C₁₄H₁₁FN₂OS: C 61.30%, H 4.04%, N 10.21%. Found: C 61.27%, H 4.25%, N
632 10.33%.

633 1-(3-benzo[d][1,3]dioxol-5-yl)-3-(1H-imidazol-1-yl)propan-1-one (**30a**). Yield: 25%.
634 Mp: 146.0-147.0 °C. IR (KBr) ν cm⁻¹: 1663 (s, ν_{C=O}). ¹H NMR (DMSO-*d*₆, 400 MHz) δ ppm:
635 7.65 (s, 1H, H_{2'}); 7.62 (dd, 1H, H₇, J₇₋₆ = 8.2 Hz, J₇₋₂ = 1.7 Hz); 7.45 (d, 1H, H₂, J₂₋₇ = 1.6 Hz);
636 7.20 (s, 1H, H_{5'}); 7.04 (d, 1H, H₆, J₆₋₇ = 8.2 Hz); 6.85 (s, 1H, H_{4'}); 6.13 (s, 2H, H₄); 4.29 (t, 2H,
637 CH₂-N, J_{CH₂-CH₂} = 6.8 Hz); 3.51 (t, 2H, CH₂-CO, J_{CH₂-CH₂} = 6.8 Hz). ¹³C NMR (DMSO-*d*₆, 100
638 MHz) δ ppm: 195.67 (CO); 151.66 (C₅); 147.85 (C₃); 137.41 (C_{2'}); 130.95 (C₁); 128.16 (C_{4'});
639 124.52 (C₇); 119.46 (C_{5'}); 108.08 (C₂); 107.32 (C₆); 102.08 (C₄); 41.35 (CH₂-N); 38.98 (CH₂-
640 CO). Anal. Calc. for C₁₃H₁₂N₂O₃: C 63.93%, H 4.95%, N 11.47%. Found: C 64.11%, H 5.26%,
641 N 11.69%.

642 1-(adamantan-1-yl)-3-(1H-imidazol-1-yl)propan-1-one (**31a**). Yield: 16%. Mp: 103.0-
643 104.0 °C. IR (KBr) ν cm⁻¹: 1696 (s, ν_{C=O}). ¹H NMR (DMSO-*d*₆, 400 MHz) δ ppm: 7.55 (s, 1H,
644 H_{2'}); 7.11 (s, 1H, H_{5'}); 6.83 (s, 1H, H_{4'}); 4.12 (t, 2H, CH₂-N, J_{CH₂-CH₂} = 6.7 Hz); 3.00 (t, 2H,
645 CH₂-CO, J_{CH₂-CH₂} = 6.7 Hz); 1.95 (s, 3H, H₃ + H₅ + H₈); 1.68-1.60 (m, 12H, H₂ + H₄ + H₆ + H₇
646 + H₉ + H₁₀). ¹³C NMR (DMSO-*d*₆, 100 MHz) δ ppm: 212.52 (CO); 137.34 (C_{2'}); 128.18 (C_{4'});
647 119.28 (C_{5'}); 45.51 (C₁); 41.03 (CH₂-N); 37.15 (3C, C₂+C₆+C₇); 36.99 (CH₂-CO); 35.93 (3C,
648 C₄+C₉+C₁₀); 27.26 (3C, C₃+C₅+C₈). Anal. Calc. for C₁₆H₂₂N₂O: C 74.38%, H 8.58%, N
649 10.84%. Found: C 74.53%, H 8.41%, N 10.76%.

650 1-([1,1'-biphenyl]-4-yl)-3-(1H-imidazol-1-yl)propan-1-one (**32a**). Yield: 18%. Mp:
651 104.0-104.5 °C. IR (KBr) ν cm⁻¹: (s, ν_{C=O}). ¹H NMR (DMSO-*d*₆, 400 MHz) δ ppm: 8.05 (d, 2H,
652 H₂ + H₆, J₂₋₃ = J₆₋₅ = 8.4 Hz); 7.82 (d, 2H, H₃ + H₅, J₃₋₂ = J₅₋₆ = 8.4 Hz); 7.74 (d, 2H, H₁₁ + H_{VI}, J<sub>II-
653 III</sub> = J_{VI-V} = 7.2 Hz); 7.68 (s, 1H, H_{2'}); 7.50 (t, 2H, H_{III} + H_V, J_{III-II} = J_{III-IV} = J_{V-IV} = J_{V-VI} = 7.4 Hz);
654 7.43 (t, 2H, H_{IV}, J_{IV-III} = J_{IV-V} = 7.3 Hz); 7.23 (s, 1H, H_{5'}); 6.87 (s, 1H, H_{4'}); 4.35 (t, 2H, CH₂-N,
655 J_{CH₂-CH₂} = 6.7 Hz); 3.62 (t, 2H, CH₂-CO, J_{CH₂-CH₂} = 6.8 Hz). ¹³C NMR (DMSO-*d*₆, 100 MHz) δ
656 ppm: 197.28 (CO); 144.81 (C₄); 138.81 (C_I); 137.48 (C_{2'}); 135.06 (C_I); 129.11 (2C, C_{III}+C_V);
657 128.72 (2C, C₂+C₆); 128.46 (C_{IV}); 128.28 (C_{4'}); 127.01 (2C, C_{II}+C_{VI}); 126.92 (2C, C₃+C₅);
658 119.47 (C_{5'}); 41.23 (CH₂-N); 39.06 (CH₂-CO). Anal. Calc. for C₁₈H₁₆N₂O: C 78.24%, H 5.84%,
659 N 10.14%. Found: C 77.99%, H 5.61%, N 10.04%.

660 3-(1H-benzo[d]imidazol-1-yl)-1-phenylpropan-1-one (**1b**). Yield: 19%. Mp: 90.5-91.5
661 °C. IR (KBr) ν cm⁻¹: 1681 (s, ν_{C=O}). ¹H NMR (DMSO-*d*₆, 400 MHz) δ ppm: 8.26 (s, 1H, H_{2'});
662 7.97 (d, 2H, H₂ + H₆, J₂₋₃ = J₆₋₅ = 7.2 Hz); 7.69 (d, 1H, H_{8'}, J_{8'-7'} = 7.9 Hz); 7.63 (t, 2H, H_{5'} + H₄,
663 J_{5'-6'} = J₄₋₃ = J₄₋₅ = 7.5 Hz); 7.50 (t, 2H, H₃ + H₅, J₃₋₂ = J₃₋₄ = J₅₋₄ = J₅₋₆ = 7.7 Hz); 7.26 (t, 1H, H_{7'},
664 J_{7'-6'} = J_{7'-8'} = 7.1 Hz); 7.20 (t, 1H, H_{6'}, J_{6'-5'} = J_{6'-7'} = 7.6 Hz); 4.62 (t, 2H, CH₂-N, J_{CH₂-CH₂} = 6.8

665 Hz); 3.69 (t, 2H, **CH₂-CO**, $J_{CH_2-CH_2} = 6.8$ Hz). ¹³C NMR (DMSO-*d*₆, 100 MHz) δ ppm: 197.77
666 (**CO**); 144.22 (**C₂**); 143.39 (**C₄**); 136.18 (**C₁**); 133.72 (**C₉**); 133.45 (**C₄**); 128.71 (2C, **C₃+C₅**);
667 127.94 (2C, **C₂+C₆**); 122.23 (**C₇**); 121.41 (**C₆**); 119.35 (**C₅**); 110.53 (**C₈**); 39.40 (**CH₂-N**);
668 38.01 (**CH₂-CO**). HRMS calculated for C₁₆H₁₄N₂O: 250.111. Found: 250.123.

669 *3-(1H-benzof[d]imidazol-1-yl)-1-(4-fluorophenyl)propan-1-one (2b)*. Yield: 20%. Mp:
670 115.5-116.5 °C. IR (KBr) ν cm⁻¹: 1684 (s, ν_{C=O}), 1233 (s, ν_{C-F}). ¹H NMR (DMSO-*d*₆, 400 MHz)
671 δ ppm: 8.25 (s, 1H, **H₂**); 8.05 (dd, 2H, **H₂ + H₆**, $J_{2-3} = J_{6-5} = 8.9$ Hz, $J_{2-F} = J_{6-F} = 5.6$ Hz); 7.68 (d,
672 1H, **H₈**, $J_{8-7} = 7.9$ Hz); 7.64 (d, 1H, **H₅**, $J_{5-6} = 7.8$ Hz); 7.33 (t, 2H, **H₃ + H₅**, $J_{3-2} = J_{3-F} = J_{5-F} =$
673 $J_{5-6} = 8.9$ Hz); 7.26 (t, 1H, **H₇**, $J_{7-6} = J_{7-8} = 7.0$ Hz); 7.19 (t, 1H, **H₆**, $J_{6-5} = J_{6-7} = 7.6$ Hz); 4.60
674 (t, 2H, **CH₂-N**, $J_{CH_2-CH_2} = 6.8$ Hz); 3.68 (t, 2H, **CH₂-CO**, $J_{CH_2-CH_2} = 6.8$ Hz). ¹³C NMR (DMSO-*d*₆,
675 100 MHz) δ ppm: 196.39 (**CO**); 165.14 (d, **C₄**, $J^I = 252.1$ Hz); 144.20 (**C₂**); 143.39 (**C₄**);
676 133.72 (**C₉**); 132.96 (d, **C₁**, $J^I = 2.7$ Hz); 130.99 (2C, **C₂+C₆**, d, $J^B = 9.5$ Hz); 122.21 (**C₇**);
677 121.41 (**C₆**); 119.34 (**C₅**); 115.71 (d, **C₃+C₅**, $J^I = 21.9$ Hz); 110.53 (**C₈**); 39.37 (**CH₂-N**); 37.99
678 (**CH₂-CO**). HRMS calculated for C₁₆H₁₃FN₂O: 268.108. Found: 268.102.

679 *3-(1H-benzof[d]imidazol-1-yl)-1-(4-chlorophenyl)propan-1-one (3b)*. Yield: 21%. Mp:
680 131.5-132.0 °C. IR (KBr) ν cm⁻¹: 1686 (s, ν_{C=O}). ¹H NMR (DMSO-*d*₆, 400 MHz) δ ppm: 8.25
681 (s, 1H, **H₂**); 7.98 (d, 2H, **H₂ + H₆**, $J_{2-3} = J_{6-5} = 8.6$ Hz); 7.68 (d, 1H, **H₈**, $J_{8-7} = 7.9$ Hz); 7.64 (d,
682 1H, **H₅**, $J_{5-6} = 7.8$ Hz); 7.57 (d, 2H, **H₃ + H₅**, $J_{3-2} = J_{5-6} = 8.6$ Hz); 7.25 (t, 1H, **H₇**, $J_{7-6} = J_{7-8} =$
683 7.6 Hz); 7.19 (t, 1H, **H₆**, $J_{6-5} = J_{6-7} = 7.6$ Hz); 4.60 (t, 2H, **CH₂-N**, $J_{CH_2-CH_2} = 6.8$ Hz); 3.68 (t,
684 2H, **CH₂-CO**, $J_{CH_2-CH_2} = 6.8$ Hz). ¹³C NMR (DMSO-*d*₆, 100 MHz) δ ppm: 197.04 (**CO**); 144.39
685 (**C₂**); 143.60 (**C₄**); 138.56 (**C₁**); 135.06 (**C₄**); 133.92 (**C₉**); 130.08 (2C, **C₂+C₆**); 129.01 (2C,
686 **C₃+C₅**); 122.42 (**C₇**); 121.61 (**C₆**); 119.55 (**C₅**); 110.73 (**C₈**); 39.52 (**CH₂-N**); 38.28 (**CH₂-**
687 **CO**). HRMS calculated for C₁₆H₁₃ClN₂O: 285.079. Found: 285.095.

688 *3-(1H-benzof[d]imidazol-1-yl)-1-(4-methoxyphenyl)propan-1-one (4b)*. Yield: 19%. Mp:
689 95.0-96.0 °C. IR (KBr) ν cm⁻¹: 1680 (s, ν_{C=O}). ¹H NMR (DMSO-*d*₆, 400 MHz) δ ppm: 8.25 (s,
690 1H, **H₂**); 7.94 (d, 2H, **H₂ + H₆**, $J_{2-3} = J_{6-5} = 8.9$ Hz); 7.68 (d, 1H, **H₈**, $J_{8-7} = 7.9$ Hz); 7.63 (d, 1H,
691 **H₅**, $J_{5-6} = 7.9$ Hz); 7.25 (t, 1H, **H₇**, $J_{7-6} = J_{7-8} = 7.0$ Hz); 7.19 (t, 1H, **H₆**, $J_{6-5} = J_{6-7} = 7.0$ Hz);
692 7.01 (d, 2H, **H₃ + H₅**, $J_{3-2} = J_{5-6} = 8.9$ Hz); 4.59 (t, 2H, **CH₂-N**, $J_{CH_2-CH_2} = 6.8$ Hz); 3.82 (s, 3H,
693 **OCH₃**); 3.61 (t, 2H, **CH₂-CO**, $J_{CH_2-CH_2} = 6.8$ Hz). ¹³C NMR (DMSO-*d*₆, 100 MHz) δ ppm:
694 196.05 (**CO**); 163.31 (**C₄**); 144.22 (**C₂**); 143.39 (**C₄**); 133.72 (**C₉**); 130.29 (2C, **C₂+C₆**); 129.20
695 (**C₁**); 122.20 (**C₇**); 121.38 (**C₆**); 119.34 (**C₅**); 113.88 (2C, **C₃+C₅**); 110.50 (**C₈**); 55.53 (**OCH₃**);
696 39.25 (**CH₂-N**); 37.60 (**CH₂-CO**). HRMS calculated for C₁₇H₁₆N₂O₂: 281.128. Found: 281.141.

697 *3-(1H-benzof[d]imidazol-1-yl)-1-(4-(trifluoromethyl)phenyl)propan-1-one (5b)*. Yield:
698 22%. Mp: 130.5-131.5 °C. IR (KBr) ν cm⁻¹: 1689 (s, ν_{C=O}), 1335 (s, ν_{C-F}), 1294 (s, ν_{C-F}), 1160
699 (s, ν_{C-F}). ¹H NMR (DMSO-*d*₆, 400 MHz) δ ppm: 8.27 (s, 1H, **H₂**); 8.16 (d, 2H, **H₂ + H₆**, $J_{2-3} =$
700 $J_{6-5} = 8.1$ Hz); 7.88 (d, 2H, **H₃ + H₅**, $J_{3-2} = J_{5-6} = 8.2$ Hz); 7.70 (d, 1H, **H₈**, $J_{8-7} = 7.8$ Hz); 7.64 (d,
701 1H, **H₅**, $J_{5-6} = 7.7$ Hz); 7.26 (t, 1H, **H₇**, $J_{7-6} = J_{7-8} = 7.0$ Hz); 7.20 (t, 1H, **H₆**, $J_{6-5} = J_{6-7} = 7.6$

702 Hz); 4.63 (t, 2H, **CH₂-N**, $J_{CH_2-CH_2} = 6.8$ Hz); 3.76 (t, 2H, **CH₂-CO**, $J_{CH_2-CH_2} = 6.8$ Hz). ¹³C NMR
703 (DMSO-*d*₆, 100 MHz) δ ppm: 197.32 (**CO**); 144.18 (**C₂**); 143.41 (**C₄**); 139.29 (**C₁**); 133.72
704 (**C₉**); 132.70 (q, **C₄**, $J^1 = 32.0$ Hz); 128.79 (2C, **C₂+C₆**); 125.68 (2C, **C₃+C₅**, q, $J^3 = 3.7$ Hz);
705 123.72 (q, **CF₃**, $J^1 = 272.7$ Hz); 122.22 (**C₇**); 121.42 (**C₆**); 119.35 (**C₅**); 110.54 (**C₈**); 39.25
706 (**CH₂-N**); 38.46 (**CH₂-CO**). HRMS calculated for C₁₇H₁₃F₃N₂O: 319.105. Found: 319.122.

707 *3-(1H-benzof[d]imidazol-1-yl)-1-(4-methylphenyl)propan-1-one (6b)*. Yield: 19%. Mp:
708 109.0-110.0 °C. IR (KBr) ν cm⁻¹: 1678 (s, ν_{C=O}). ¹H NMR (DMSO-*d*₆, 400 MHz) δ ppm: 8.25
709 (s, 1H, **H₂**); 7.86 (d, 2H, **H₂ + H₆**, $J_{2,3} = J_{6,5} = 8.2$ Hz); 7.68 (d, 1H, **H₈**, $J_{8,7} = 7.8$ Hz); 7.64 (d,
710 1H, **H₅**, $J_{5,6} = 7.7$ Hz); 7.30 (d, 2H, **H₃ + H₅**, $J_{3,2} = J_{5,6} = 8.0$ Hz); 7.25 (t, 1H, **H₇**, $J_{7,6} = J_{7,8} =$
711 7.0 Hz); 7.19 (t, 1H, **H₆**, $J_{6,5} = J_{6,7} = 7.6$ Hz); 4.60 (t, 2H, **CH₂-N**, $J_{CH_2-CH_2} = 6.8$ Hz); 3.64 (t,
712 2H, **CH₂-CO**, $J_{CH_2-CH_2} = 6.8$ Hz); 2.35 (s, 3H, **CH₃**). ¹³C NMR (DMSO-*d*₆, 100 MHz) δ ppm:
713 197.74 (**CO**); 144.70 (**C₂**); 144.35 (**C₄**); 143.88 (**C₄**); 134.25 (**C₁**); 134.20 (**C₉**); 129.73 (2C,
714 **C₃+C₅**); 128.54 (2C, **C₂+C₆**); 122.70 (**C₇**); 121.88 (**C₆**); 119.83 (**C₅**); 111.00 (**C₈**); 39.93 (**CH₂-**
715 **N**); 38.36 (**CH₂-CO**); 21.60 (**CH₃**). HRMS calculated for C₁₇H₁₆N₂O: 265.134. Found: 265.149.

716 *3-(1H-benzof[d]imidazol-1-yl)-1-(4-nitrophenyl)propan-1-one (7b)*. Yield: 22%. Mp:
717 153.0-154.0 °C. IR (KBr) ν cm⁻¹: 1689 (s, ν_{C=O}), 1521 (s, ν_{NO₂}), 1348 (s, ν_{NO₂}). ¹H NMR
718 (DMSO-*d*₆, 400 MHz) δ ppm: 8.31 (d, 2H, **H₃ + H₅**, $J_{3,2} = J_{5,6} = 8.9$ Hz); 8.26 (s, 1H, **H₂**); 8.19
719 (d, 2H, **H₂ + H₆**, $J_{2,3} = J_{6,5} = 8.9$ Hz); 7.70 (d, 1H, **H₈**, $J_{8,7} = 7.9$ Hz); 7.64 (d, 1H, **H₅**, $J_{5,6} = 7.8$
720 Hz); 7.26 (t, 1H, **H₇**, $J_{7,6} = J_{7,8} = 7.0$ Hz); 7.20 (t, 1H, **H₆**, $J_{6,5} = J_{6,7} = 7.0$ Hz); 4.63 (t, 2H,
721 **CH₂-N**, $J_{CH_2-CH_2} = 6.8$ Hz); 3.78 (t, 2H, **CH₂-CO**, $J_{CH_2-CH_2} = 6.8$ Hz). ¹³C NMR (DMSO-*d*₆, 100
722 MHz) δ ppm: 197.07 (**CO**); 150.02 (**C₄**); 144.17 (**C₂**); 143.40 (**C₄**); 140.68 (**C₁**); 133.71 (**C₉**);
723 129.40 (2C, **C₂+C₆**); 123.79 (2C, **C₃+C₅**); 122.23 (**C₇**); 121.44 (**C₆**); 119.36 (**C₅**); 110.55 (**C₈**);
724 39.22 (**CH₂-N**); 38.71 (**CH₂-CO**). HRMS calculated for C₁₆H₁₃N₃O₃: 296.103. Found: 296.121.

725 *3-(1H-benzof[d]imidazol-1-yl)-1-(thiophen-3-yl)propan-1-one (8b)*. Yield: 24%. Mp:
726 125.5-126.5 °C. IR (KBr) ν cm⁻¹: 1674 (s, ν_{C=O}). ¹H NMR (DMSO-*d*₆, 400 MHz) δ ppm: 8.51
727 (dd, 1H, **H₂**, $J_{2,4} = 1.7$ Hz); 8.24 (s, 1H, **H₂**); 7.67 (d, 1H, **H₈**, $J_{8,7} = 7.9$ Hz); 7.63 (d, 1H, **H₅**,
728 $J_{5,6} = 8.1$ Hz); 7.61 (dd, 1H, **H₅**, $J_{5,4} = 5.3$ Hz, $J_{5,2} = 3$ Hz); 7.50 (d, 1H, **H₄**, $J_{4,5} = 5.0$ Hz); 7.26
729 (t, 1H, **H₇**, $J_{7,6} = J_{7,8} = 7.3$ Hz); 7.19 (t, 1H, **H₆**, $J_{6,5} = J_{6,7} = 7.4$ Hz); 4.59 (t, 2H, **CH₂-N**,
730 $J_{CH_2-CH_2} = 6.8$ Hz); 3.58 (t, 2H, **CH₂-CO**, $J_{CH_2-CH_2} = 6.8$ Hz). ¹³C NMR (DMSO-*d*₆, 100 MHz) δ
731 ppm: 192.08 (**CO**); 144.18 (**C₂**); 143.38 (**C₄**); 141.46 (**C₃**); 134.11 (**C₂**); 133.67 (**C₉**); 127.54
732 (**C₅**); 126.34 (**C₄**); 122.22 (**C₇**); 121.40 (**C₆**); 119.35 (**C₅**); 110.50 (**C₈**); 39.27 (**CH₂-N**); 39.04
733 (**CH₂-CO**). Anal. HRMS calculated for C₁₄H₁₂N₂OS: 257.092. Found: 257.090.

734 *3-(1H-benzof[d]imidazol-1-yl)-1-(thiophen-2-yl)propan-1-one (9b)*. Yield: 23%. Mp:
735 115.0-116.0 °C. IR (KBr) ν cm⁻¹: 1666 (s, ν_{C=O}). ¹H NMR (DMSO-*d*₆, 400 MHz) δ ppm: 8.23
736 (s, 1H, **H₂**); 7.99 (dd, 1H, **H₅**, $J_{5,4} = 4.9$ Hz, $J_{5,3} = 1.1$ Hz); 7.95 (dd, 1H, **H₃**, $J_{3,4} = 3.8$ Hz, $J_{3,5} =$
737 1.1 Hz); 7.67 (d, 1H, **H₈**, $J_{8,7} = 7.9$ Hz); 7.63 (d, 1H, **H₅**, $J_{5,6} = 7.9$ Hz); 7.26 (td, 1H, **H₇**, $J_{7,6}$
738 $= J_{7,8} = 7.8$ Hz, $J_{7,5} = 1.1$ Hz); 7.22-7.17 (m, 2H, **H₆** + **H₄**); 4.60 (t, 2H, **CH₂-N**, $J_{CH_2-CH_2} = 6.8$

739 Hz); 3.62 (t, 2H, **CH₂-CO**, $J_{CH_2-CH_2} = 6.8$ Hz). ¹³C NMR (DMSO-*d*₆, 100 MHz) δ ppm: 190.75
740 (**CO**); 144.18 (**C₂**); 143.36 (**C₂**); 143.25 (**C₄**); 135.17 (**C₅**); 133.79 (**C₉**); 133.66 (**C₃**); 128.76
741 (**C₄**); 122.28 (**C₇**); 121.45 (**C₆**); 119.36 (**C₅**); 110.51 (**C₈**); 39.38 (**CH₂-N**); 38.39 (**CH₂-CO**).
742 HRMS calculated for C₁₄H₁₂N₂OS: 257.092. Found: 257.093.

743 *3-(1H-benzof[d]imidazol-1-yl)-1-(furan-2-yl)propan-1-one (10b)*. Yield: 25%. Mp:
744 86.5-87.5 °C. IR (KBr) ν cm⁻¹: 1669.89 (s, ν_{C=O}). ¹H NMR (DMSO-*d*₆, 400 MHz) δ ppm: 8.21
745 (s, 1H, **H₂**); 7.97 (d, 1H, **H₅**, $J_{5-4} = 1.1$ Hz); 7.66 (d, 1H, **H₈**, $J_{8-7} = 7.9$ Hz); 7.63 (d, 1H, **H₅**, J_{5-6}
746 $= 7.9$ Hz); 7.47 (d, 1H, **H₃**, $J_{3-4} = 3.3$ Hz); 7.26 (td, 1H, **H₇**, $J_{7-6} = J_{7-8} = 7.7$ Hz, $J_{7-5} = 1.2$
747 Hz); 7.19 (t, 1H, **H₆**, $J_{6-5} = J_{6-7} = 7.5$ Hz); 6.68 (dd, 1H, **H₄**, $J_{4-3} = 3.6$ Hz, $J_{4-5} = 1.7$ Hz); 4.59 (t,
748 2H, **CH₂-N**, $J_{CH_2-CH_2} = 6.8$ Hz); 3.46 (t, 2H, **CH₂-CO**, $J_{CH_2-CH_2} = 6.8$ Hz). ¹³C NMR (DMSO-*d*₆,
749 100 MHz) δ ppm: 185.87 (**CO**); 151.52 (**C₂**); 147.98 (**C₅**); 144.15 (**C₂**); 143.36 (**C₄**); 133.61
750 (**C₉**); 122.27 (**C₇**); 121.44 (**C₆**); 119.37 (**C₅**); 118.93 (**C₃**); 112.53 (**C₄**); 110.45 (**C₈**); 38.85
751 (**CH₂-N**); 37.72 (**CH₂-CO**). HRMS calculated for C₁₄H₁₂N₂O₂: 241.097. Found: 241.113.

752 *3-(1H-benzof[d]imidazol-1-yl)-1-(naphthalene-2-yl)propan-1-one (11b)*. Yield: 27%.
753 Mp: 159.0-160.0 °C. IR (KBr) ν cm⁻¹: 1685.13 (s, ν_{C=O}). ¹H NMR (DMSO-*d*₆, 400 MHz) δ ppm:
754 8.68 (s, 1H, **H₁**); 8.31 (s, 1H, **H₂**); 8.07 (d, 1H, **H₃**, $J_{3-4} = 7.9$ Hz); 7.99-7.96 (m, 3H, **H₄ + H₆ +**
755 **H₉**); 7.73 (d, 1H, **H₈**, $J_{8-7} = 7.9$ Hz); 7.67-7.58 (m, 3H, **H₇ + H₈ + H₅**); 7.27 (t, 1H, **H₇**, $J_{7-6} =$
756 $J_{7-8} = 7.1$ Hz); 7.21 (t, 1H, **H₆**, $J_{6-5} = J_{6-7} = 7.0$ Hz); 4.68 (t, 2H, **CH₂-N**, $J_{CH_2-CH_2} = 6.9$ Hz);
757 3.83 (t, 2H, **CH₂-CO**, $J_{CH_2-CH_2} = 6.9$ Hz). ¹³C NMR (DMSO-*d*₆, 100 MHz) δ ppm: 197.70;
758 144.27; 143.46; 135.14; 133.77; 133.46; 132.15; 130.19; 129.59; 128.74; 128.30; 127.65;
759 126.95; 123.29; 122.27; 121.46; 119.39; 110.60; 39.57; 38.19. HRMS calculated for C₂₀H₁₆N₂O:
760 301.134. Found: 301.153.

761 *1-(benzo[b]thiophen-3-yl)-3-(1H-benzof[d]imidazol-1-yl)propan-1-one (12b)*. Yield:
762 19%. Mp: 175.0-176.0 °C. IR (KBr) ν cm⁻¹: 1663.89 (s, ν_{C=O}). ¹H NMR (DMSO-*d*₆, 400 MHz)
763 δ ppm: 8.98 (s, 1H, **H₂**); 8.62 (d, 1H, **H₈**, $J_{8-7} = 7.7$ Hz); 8.28 (s, 1H, **H₂**); 8.07 (d, 1H, **H₅**, $J_{5-6} =$
764 7.8 Hz); 7.71 (d, 1H, **H₈**, $J_{8-7} = 8.0$ Hz); 7.64 (d, 2H, **H₅**, $J_{5-6} = 7.9$ Hz); 7.53-7.43 (m, 2H, **H₆**
765 **+ H₇**); 7.28-7.18 (m, 2H, **H₆ + H₇**); 4.66 (t, 2H, **CH₂-N**, $J_{CH_2-CH_2} = 6.9$ Hz); 3.72 (t, 2H, **CH₂-**
766 **CO**, $J_{CH_2-CH_2} = 6.9$ Hz). ¹³C NMR (DMSO-*d*₆, 100 MHz) δ ppm: 193.19 (**CO**); 144.20 (**C₂**);
767 143.41 (**C₄**); 140.21 (**C₂**); 139.33 (**C₃**); 136.07 (**C₄**); 133.76 (**C₉**); 133.72 (**C₉**); 125.81 (**C₆**);
768 125.38 (**C₇**); 124.61 (**C₈**); 122.89 (**C₅**); 122.25 (**C₇**); 121.43 (**C₆**); 119.37 (**C₅**); 110.54 (**C₈**);
769 39.45 (**CH₂-N**); 39.39 (**CH₂-CO**). HRMS calculated for C₁₈H₁₄N₂OS: 307.108. Found: 307.107.

770 *1-(benzo[b]thiophen-2-yl)-3-(1H-benzof[d]imidazol-1-yl)propan-1-one (13b)*. Yield:
771 21%. Mp: 169.0-170.0 °C. IR (KBr) ν cm⁻¹: 1665.26 (s, ν_{C=O}). ¹H NMR (DMSO-*d*₆, 400 MHz)
772 δ ppm: 8.38 (s, 1H, **H₃**); 8.26 (s, 1H, **H₂**); 8.04 (d, 1H, **H₅**, $J_{5-6} = 8.1$ Hz); 7.98 (d, 1H, **H₈**, $J_{8-7} =$
773 7.9 Hz); 7.71 (d, 1H, **H₈**, $J_{8-7} = 8.0$ Hz); 7.64 (d, 1H, **H₅**, $J_{5-6} = 7.9$ Hz); 7.53 (t, 1H, **H₆**, $J_{6-5} =$
774 $J_{6-7} = 7.0$ Hz); 7.46 (t, 1H, **H₇**, $J_{7-8} = J_{7-6} = 7.1$ Hz); 7.27 (t, 1H, **H₇**, $J_{7-6} = J_{7-8} = 7.2$ Hz); 7.20 (t,
775 1H, **H₆**, $J_{6-5} = J_{6-7} = 7.1$ Hz); 4.65 (t, 2H, **CH₂-N**, $J_{CH_2-CH_2} = 6.8$ Hz); 3.75 (t, 2H, **CH₂-CO**, J_{CH_2-}

776 $_{CH_2} = 6.8$ Hz). ^{13}C NMR (DMSO- d_6 , 100 MHz) δ ppm: 192.54 (CO); 144.22 (C_{2'}); 143.40 (C_{4'});
777 142.54 (C₂); 141.50 (C₄); 139.06 (C₉); 133.68 (C_{9'}); 131.31 (C₃); 127.85 (C₆); 126.35 (C₈);
778 125.31 (C₇); 123.17 (C₅); 122.31 (C₇); 121.49 (C_{6'}); 119.39 (C_{5'}); 110.58 (C_{8'}); 39.41 (CH₂-N);
779 38.41 (CH₂-CO). HRMS calculated for C₁₈H₁₄N₂O₅: 307.108. Found: 307.196.

780 *3-(1H-imidazol-1-yl)-1-(benzofuran-2-yl)propan-1-one (14b)*. Yield: 21%. Mp: 157.0-
781 158.0 °C. IR (KBr) ν cm⁻¹: 1680.14 (s, $\nu_{C=O}$). 1H NMR (DMSO- d_6 , 400 MHz) δ ppm: 8.26 (s,
782 1H, H_{2'}); 7.93 (s, 1H, H₃); 7.81 (d, 1H, H₅, $J_{5-6} = 7.8$ Hz); 7.73-7.67 (m, 2H, H₈ + H_{8'}); 7.64 (d,
783 1H, H_{5'}, $J_{5'-6'} = 8.0$ Hz); 7.54 (ddd, 1H, H₇, $J_{7-8} = 8.4$ Hz, $J_{7-6} = 7.3$ Hz, $J_{7-5} = 1.2$ Hz); 7.36 (t, 1H,
784 H₆, $J_{6-5} = J_{6-7} = 7.2$ Hz); 7.28 (t, 1H, H_{7'}, $J_{7'-6'} = J_{7'-8'} = 7.1$ Hz); 7.20 (t, 1H, H_{6'}, $J_{6'-5'} = J_{6'-7'} = 7.0$
785 Hz); 4.66 (t, 2H, CH₂-N, $J_{CH_2-CH_2} = 6.8$ Hz); 3.64 (t, 2H, CH₂-CO, $J_{CH_2-CH_2} = 6.8$ Hz). ^{13}C NMR
786 (DMSO- d_6 , 100 MHz) δ ppm: 188.11 (CO); 154.97 (C₉); 151.61 (C₂); 144.20 (C_{2'}); 143.40
787 (C_{4'}); 133.66 (C_{9'}); 128.65 (C₇); 126.69 (C₄); 124.11 (C₆); 123.74 (C₅); 122.32 (C_{7'}); 121.50
788 (C_{6'}); 119.41 (C_{5'}); 114.50 (C₃); 112.26 (C₈); 110.54 (C_{8'}); 38.88 (CH₂-N); 38.26 (CH₂-CO).
789 HRMS calculated for C₁₈H₁₄N₂O₂: 291.113. Found: 291.131.

790 *3-(1H-benzofur[2,3-b]imidazol-1-yl)-1-(3,5-dimethoxyphenyl)propan-1-one (15b)*. Yield:
791 24%. Mp: 160.0-161.0 °C. IR (KBr) ν cm⁻¹: 1685.35 (s, $\nu_{C=O}$). 1H NMR (DMSO- d_6 , 400 MHz)
792 δ ppm: 8.25 (s, 1H, H_{2'}); 7.68 (d, 1H, H_{8'}, $J_{8'-7'} = 7.9$ Hz); 7.63 (d, 1H, H_{5'}, $J_{5'-6'} = 7.9$ Hz); 7.26
793 (t, 1H, H_{7'}, $J_{7'-6'} = J_{7'-8'} = 7.0$ Hz); 7.19 (t, 1H, H_{6'}, $J_{6'-5'} = J_{6'-7'} = 7.0$ Hz); 7.07 (d, 2H, H₂ + H₆, J_{2-4}
794 = $J_{6-4} = 2.3$ Hz); 6.75 (t, 1H, H₄, $J_{4-2} = J_{4-6} = 2.2$ Hz); 4.59 (t, 2H, CH₂-N, $J_{CH_2-CH_2} = 6.7$ Hz); 3.77
795 (s, 6H, OCH₃); 3.67 (t, 2H, CH₂-CO, $J_{CH_2-CH_2} = 6.7$ Hz). ^{13}C NMR (DMSO- d_6 , 100 MHz) δ
796 ppm: 197.54 (CO); 160.59 (2C, C₃+C₅); 144.25 (C_{2'}); 143.38 (C_{4'}); 138.25 (C₁); 133.75 (C_{9'});
797 122.24 (C_{7'}); 121.43 (C_{6'}); 119.35 (C_{5'}); 110.58 (C_{8'}); 105.67 (2C, C₂+C₆); 105.42 (C₄); 55.52
798 (2C, OCH₃); 39.45 (CH₂-N); 38.22 (CH₂-CO). HRMS calculated for C₁₈H₁₈N₂O₃: 311.139.
799 Found: 311.159.

800 *1-(3-benzofur[2,3-b]imidazol-5-yl)-3-(1H-benzofur[2,3-b]imidazol-1-yl)propan-1-one (16b)*.
801 Yield: 22%. Mp: 132.5-133.5 °C. IR (KBr) ν cm⁻¹: 1675.26 (s, $\nu_{C=O}$). 1H NMR (DMSO- d_6 , 400
802 MHz) δ ppm: 8.24 (s, 1H, H_{2'}); 7.68-7.59 (m, 3H, H₇ + H_{5'} + H_{8'}); 7.45 (d, 1H, H₂, $J_{2-7} = 1.6$
803 Hz); 7.25 (t, 1H, H_{7'}, $J_{7'-6'} = J_{7'-8'} = 7.1$ Hz); 7.19 (t, 1H, H_{6'}, $J_{6'-5'} = J_{6'-7'} = 7.0$ Hz); 7.00 (d, 1H,
804 H₆, $J_{6-7} = 8.2$ Hz); 6.12 (s, 2H, H₄); 4.58 (t, 2H, CH₂-N, $J_{CH_2-CH_2} = 6.8$ Hz); 3.60 (t, 2H, CH₂-CO,
805 $J_{CH_2-CH_2} = 6.8$ Hz). ^{13}C NMR (DMSO- d_6 , 100 MHz) δ ppm: 195.75 (CO); 151.66 (C₅); 147.84
806 (C₃); 144.23 (C_{2'}); 143.39 (C_{4'}); 133.73 (C_{9'}); 130.91 (C₁); 124.53 (C₇); 122.23 (C_{7'}); 121.42
807 (C_{6'}); 119.35 (C_{5'}); 110.55 (C_{8'}); 108.06 (C₆); 107.33 (C₂); 102.07 (C₄); 39.29 (CH₂-N); 37.76
808 (CH₂-CO). HRMS calculated for C₁₇H₁₄N₂O₃: 295.108. Found: 295.126.

809 *1-(adamantan-1-yl)-3-(1H-benzofur[2,3-b]imidazol-1-yl)propan-1-one (17b)*. Yield: 20%.
810 Mp: 114.5-115.5 °C. IR (KBr) ν cm⁻¹: 1695 (s, $\nu_{C=O}$). 1H NMR (DMSO- d_6 , 400 MHz) δ ppm:
811 8.15 (s, 1H, H_{2'}); 7.63-7.60 (m, 2H, H_{5'} + H_{8'}); 7.25 (t, 1H, H_{7'}, $J_{7'-6'} = J_{7'-8'} = 7.2$ Hz); 7.18 (t,
812 1H, H_{6'}, $J_{6'-5'} = J_{6'-7'} = 7.1$ Hz); 4.41 (t, 2H, CH₂-N, $J_{CH_2-CH_2} = 6.7$ Hz); 3.10 (t, 2H, CH₂-CO, J_{CH_2-}

813 $_{CH_2} = 6.7$ Hz); 1.92 (s, 3H, **H**₃ + **H**₅ + **H**₈); 1.68-1.56 (m, 12H, **H**₂ + **H**₄ + **H**₆ + **H**₇ + **H**₉ + **H**₁₀).
814 ¹³C NMR (DMSO-*d*₆, 100 MHz) δ ppm: 213.18 (**CO**); 144.59 (**C**_{2'}); 143.81 (**C**_{4'}); 134.11 (**C**_{9'});
815 122.67 (**C**_{7'}); 121.83 (**C**_{6'}); 119.82 (**C**_{5'}); 110.91 (**C**_{8'}); 46.02 (**C**₁); 39.72 (**CH**₂-**N**); 37.64 (3C,
816 **C**₂+**C**₆+**C**₇); 36.37 (3C, **C**₄+**C**₉+**C**₁₀); 36.11 (**CH**₂-**CO**); 27.71 (3C, **C**₃+**C**₅+**C**₈). HRMS
817 calculated for C₂₀H₂₄N₂O: 309.196. Found: 309.215.

818 *1-(4-fluorophenyl)-3-(2-nitro-1H-imidazol-1-yl)propan-1-one (1c)*. Yield: 21%. Mp:
819 92.5-93.5 °C. IR (KBr) ν cm⁻¹: 1679 (s, ν_{C=O}), 1532 (s, ν_{NO2}), 1362 (s, ν_{NO2}), 1216 (s, ν_{C-F}). ¹H
820 NMR (DMSO-*d*₆, 400 MHz) δ ppm: 8.05 (dd, 2H, **H**₂ + **H**₆, $J_{2,3} = J_{6,5} = 8.9$ Hz, $J_{2,F} = J_{6,F} = 5.5$
821 Hz); 7.70 (d, 1H, **H**_{5'}, $J_{5',4'} = 0.9$ Hz); 7.35 (t, 2H, **H**₃ + **H**₅, $J_{3,2} = J_{5,6} = 8.9$ Hz); 7.16 (d, 1H, **H**_{4'},
822 $J_{4',5'} = 0.9$ Hz); 4.74 (t, 2H, **CH**₂-**N**, $J_{CH_2-CH_2} = 6.8$ Hz); 3.70 (t, 2H, **CH**₂-**CO**, $J_{CH_2-CH_2} = 6.8$ Hz).
823 ¹³C NMR (DMSO-*d*₆, 100 MHz) δ ppm: 196.09; 165.21 (d, ¹*J* = 252.1 Hz); 144.85; 132.79 (d,
824 ⁴*J* = 2.8 Hz); 131.04 (2C, d, ³*J* = 9.5 Hz); 127.99; 127.61; 115.75 (2C, d, ²*J* = 21.9 Hz); 44.59;
825 39.49. Anal. Calc. for C₁₂H₁₀FN₃O₃: C 54.76%, H 3.83%, N 15.96%. Found: C 54.72%, H
826 3.93%, N 15.69%.

827 *1-(4-chlorophenyl)-3-(2-nitro-1H-imidazol-1-yl)propan-1-one (2c)* Yield: 23%. Mp:
828 113.5-114.5 °C. IR (KBr) ν cm⁻¹: 1680 (s, ν_{C=O}), 1540 (s, ν_{NO2}), 1352 (s, ν_{NO2}). ¹H NMR
829 (DMSO-*d*₆, 400 MHz) δ ppm: 7.98 (d, 2H, **H**₂ + **H**₆, $J_{2,3} = J_{6,5} = 8.6$ Hz); 7.70 (d, 1H, **H**_{5'}, $J_{5',4'} =$
830 0.9 Hz); 7.60 (d, 2H, **H**₃ + **H**₅, $J_{3,2} = J_{5,6} = 8.6$ Hz); 7.16 (d, 1H, **H**_{4'}, $J_{4',5'} = 0.9$ Hz); 4.74 (t, 2H,
831 **CH**₂-**N**, $J_{CH_2-CH_2} = 6.7$ Hz); 3.70 (t, 2H, **CH**₂-**CO**, $J_{CH_2-CH_2} = 6.7$ Hz). ¹³C NMR (DMSO-*d*₆, 100
832 MHz) δ ppm: 196.55; 144.86; 138.47; 134.70; 130.45; 129.92 (2C); 129.00; 128.85 (2C);
833 128.00; 127.61; 44.54; 38.55. Anal. Calc. for C₁₂H₁₀ClN₃O₃: C 51.53%, H 3.60%, N 15.02%.
834 Found: C 51.55%, H 3.69%, N 14.91%.

835 *1-(4-methoxyphenyl)-3-(2-nitro-1H-imidazol-1-yl)propan-1-one (3c)* Yield: 16%. Mp:
836 140.5-141.5 °C. IR (KBr) ν cm⁻¹: 1665 (s, ν_{C=O}), 1532 (s, ν_{NO2}), 1354 (s, ν_{NO2}). ¹H NMR
837 (DMSO-*d*₆, 400 MHz) δ ppm: 7.95 (d, 2H, **H**₂ + **H**₆, $J_{2,3} = J_{6,5} = 8.9$ Hz); 7.70 (s, 1H, **H**_{5'}); 7.16
838 (s, 1H, **H**_{4'}); 7.04 (d, 2H, **H**₃ + **H**₅, $J_{3,2} = J_{5,6} = 8.9$ Hz); 4.73 (t, 2H, **CH**₂-**N**, $J_{CH_2-CH_2} = 6.8$ Hz);
839 3.84 (s, 3H, **OCH**₃); 3.63 (t, 2H, **CH**₂-**CO**, $J_{CH_2-CH_2} = 6.8$ Hz). ¹³C NMR (DMSO-*d*₆, 100 MHz) δ
840 ppm: 195.75; 163.41; 130.34 (2C); 129.01; 127.95; 127.62; 113.92 (2C); 55.57; 44.77; 38.16.
841 Anal. Calc. for C₁₃H₁₃N₃O₄: C 56.72%, H 4.76%, N 15.27%. Found: C 56.55%, H 4.74%, N
842 15.72%.

843 *1-(benzo[*b*]thiophen-3-yl)-3-(2-nitro-1H-imidazol-1-yl)propan-1-one (4c)*. Yield: 23%.
844 Mp: 138.0-139.0 °C. IR (KBr) ν cm⁻¹: 1663 (s, ν_{C=O}), 1532 (s, ν_{NO2}), 1351 (s, ν_{NO2}). ¹H NMR
845 (DMSO-*d*₆, 400 MHz) δ ppm: 8.99 (s, 1H, **H**₂); 8.59 (dt, 1H, **H**₅, $J_{5,6} = 8.2$ Hz, $J_{5,8} = 0.9$ Hz);
846 8.09 (dt, 1H, **H**₈, $J_{8,7} = 7.8$ Hz, $J_{8,5} = 0.9$ Hz); 7.73 (d, 1H, **H**_{5'}, $J_{5',4'} = 1.1$ Hz); 7.54-7.17 (m, 2H,
847 **H**₆+**H**₇); 7.17 (d, 1H, **H**_{4'}, $J_{4',5'} = 1.0$ Hz); 4.79 (t, 2H, **CH**₂-**N**, $J_{CH_2-CH_2} = 6.8$ Hz); 3.73 (t, 2H,
848 **CH**₂-**CO**, $J_{CH_2-CH_2} = 6.8$ Hz). ¹³C NMR (DMSO-*d*₆, 100 MHz) δ ppm: 192.82; 140.45; 139.37;

849 136.06; 133.58; 128.09; 127.71; 125.89; 125.46; 124.59; 122.98; 44.71; 39.82. Anal. Calc. for
850 C₁₄H₁₁N₃O₃S: C 55.81%, H 3.68%, N 13.95%. Found: C 55.59%, H 3.93%, N 13.86%.

851 *1-(4-fluorophenyl)-3-(2-methyl-1H-imidazol-1-yl)propan-1-one (1d)*. Yield: 21%. Mp:
852 117.0-117.5 °C. IR (KBr) ν cm⁻¹: 1673 (s, $\nu_{C=O}$). ¹H NMR (CDCl₃, 400 MHz) δ ppm: 7.95-7.91
853 (m, 2H, **H₂ + H₆**); 7.13 (t, 2H, **H₃ + H₅**, $J_{3-2} = J_{5-6} = 8.6$ Hz); 6.87 (dd, 2H, **H₄ + H_{5'}**, $J_{4'-5'} = J_{5'-4'} =$
854 6.0 Hz, $J_{4'-CH_3} = J_{5'-CH_3} = 1.2$ Hz); 4.30 (t, 2H, **CH₂-N**, $J_{CH_2-CH_2} = 6.8$ Hz); 3.35 (t, 2H, **CH₂-CO**,
855 $J_{CH_2-CH_2} = 6.8$ Hz); 2.42 (s, 3H, **CH₃-Amine**). ¹³C NMR (CDCl₃, 100 MHz) δ ppm: 195.18;
856 166.18 (d, $^1J = 255.8$ Hz); 144.60; 132.75 (d, $^4J = 2.9$ Hz); 130.76 (2C, d, $^3J = 9.4$ Hz); 127.70;
857 119.18; 116.09 (2C, d, $^2J = 21.8$ Hz); 40.70; 39.33; 13.20. Anal. Calc. for C₁₃H₁₃FN₂O: C
858 67.23%, H 5.64%, N 12.06%. Found: C 67.58%, H 5.94%, N 12.09%.

859 *1-(4-chlorophenyl)-3-(2-methyl-1H-imidazol-1-yl)propan-1-one (2d)* Yield: 14%. Mp:
860 144.0-145.0 °C. IR (KBr) ν cm⁻¹: 1674 (s, $\nu_{C=O}$). ¹H NMR (CDCl₃, 400 MHz) δ ppm: 7.84 (d,
861 2H, **H₂ + H₆**, $J_{2-3} = J_{6-5} = 8.6$ Hz); 7.44 (d, 2H, **H₃ + H₅**, $J_{3-2} = J_{5-6} = 8.6$ Hz); 6.88 (d, 2H, **H₄ +**
862 **H_{5'}**, $J_{4'-5'} = J_{5'-4'} = 7.0$ Hz); 4.31 (t, 2H, **CH₂-N**, $J_{CH_2-CH_2} = 6.8$ Hz); 3.35 (t, 2H, **CH₂-CO**, $J_{CH_2-CH_2}$
863 = 6.8 Hz); 2.42 (s, 3H, **CH₃-Amine**). ¹³C NMR (CDCl₃, 100 MHz) δ ppm: 195.60; 144.62;
864 140.42; 134.60; 129.49 (2C); 129.29 (2C); 127.75; 119.18; 40.67; 39.42; 13.22. Anal. Calc. for
865 C₁₃H₁₃ClN₂O: C 62.78%, H 5.27%, N 11.26%. Found: C 62.55%, H 5.41%, N 11.22%.

866 *1-(4-methoxyphenyl)-3-(2-methyl-1H-imidazol-1-yl)propan-1-one (3d)* Yield: 20%. Mp:
867 104.0-105.0 °C. IR (KBr) ν cm⁻¹: 1666 (s, $\nu_{C=O}$). ¹H NMR (DMSO-*d*₆, 400 MHz) δ ppm: 7.95
868 (d, 2H, **H₂ + H₆**, $J_{2-3} = J_{6-5} = 9.0$ Hz); 7.07 (d, 1H, **H_{5'}**, $J_{5'-CH_3} = 1.3$ Hz); 7.03 (d, 2H, **H₃ + H₅**, J_{3-2}
869 = $J_{5-6} = 8.9$ Hz); 6.68 (d, 1H, **H_{4'}**, $J_{4'-CH_3} = 1.3$ Hz); 4.19 (t, 2H, **CH₂-N**, $J_{CH_2-CH_2} = 6.9$ Hz); 3.84
870 (s, 3H, **OCH₃**); 3.46 (t, 2H, **CH₂-CO**, $J_{CH_2-CH_2} = 6.9$ Hz); 2.31 (s, 3H, **CH₃-Amine**). ¹³C NMR
871 (DMSO-*d*₆, 100 MHz) δ ppm: 196.07; 163.32; 143.84; 130.34 (2C); 129.28; 126.27; 119.38;
872 113.91 (2C); 55.57; 40.47; 38.52; 12.64. Anal. Calc. for C₁₄H₁₆N₂O₂: C 68.83%, H 6.60%, N
873 11.47%. Found: C 68.73%, H 6.49%, N 11.86%.

874 *1-(benzo[*b*]thiophen-3-yl)-3-(2-methyl-1H-imidazol-1-yl)propan-1-one (4d)*. Yield:
875 16%. Mp: 113.0-114.0 °C. IR (KBr) ν cm⁻¹: 1655 (s, $\nu_{C=O}$). ¹H NMR (CDCl₃, 400 MHz) δ ppm:
876 8.74 (d, 1H, **H₅**, $J_{5-6} = 8.2$ Hz); 8.21 (s, 1H, **H₂**); 7.87 (d, 1H, **H₈**, $J_{8-7} = 8.0$ Hz); 7.51 (t, 1H, **H₆**,
877 $J_{6-7} = 7.6$ Hz); 7.44 (t, 1H, **H₇**, $J_{7-6} = 7.6$ Hz); 6.90 (d, 2H, **H₄' + H_{5'}**, $J_{4'-CH_3} = J_{5'-CH_3} = 1.6$ Hz);
878 4.36 (t, 2H, **CH₂-N**, $J_{CH_2-CH_2} = 6.8$ Hz); 3.41 (t, 2H, **CH₂-CO**, $J_{CH_2-CH_2} = 6.8$ Hz); 2.44 (s, 3H,
879 **CH₃-Amine**). ¹³C NMR (CDCl₃, 100 MHz) δ ppm: 191.73; 144.64; 139.92; 137.43; 136.39;
880 134.78; 127.73; 126.22; 125.87; 125.63; 122.47; 119.22; 40.85; 40.82; 13.23. Anal. Calc. for
881 C₁₅H₁₄N₂OS: C 66.64%, H 5.22%, N 10.36%. Found: C 67.04%, H 5.34%, N 10.32%.

882 *1-(4-fluorophenyl)-3-(4-nitro-1H-imidazol-1-yl)propan-1-one (1e)*. Yield: 22%. Mp:
883 137.5-138.5 °C. IR (KBr) ν cm⁻¹: 1684 (s, $\nu_{C=O}$), 1520 (s, ν_{NO_2}), 1335 (s, ν_{NO_2}). ¹H NMR
884 (DMSO-*d*₆, 400 MHz) δ ppm: 8.46 (d, 1H, **H_{5'}**, $J_{5'-2'} = 1.5$ Hz); 8.07 (dd, 2H, **H₂ + H₆**, $J_{2-3} = J_{6-5} =$
885 8.8 Hz, $J_{2-F} = J_{6-F} = 5.6$ Hz); 7.91 (d, 1H, **H_{2'}**, $J_{2'-5'} = 1.4$ Hz); 7.37 (t, 2H, **H₃ + H₅**, $J_{3-2} = J_{5-6} = 8.8$

886 Hz); 4.43 (t, 2H, **CH₂-N**, $J_{CH_2-CH_2} = 6.8$ Hz); 3.73 (t, 2H, **CH₂-CO**, $J_{CH_2-CH_2} = 6.8$ Hz). ¹³C NMR
887 (DMSO-*d*₆, 100 MHz) δ ppm: 195.99; 165.24 (d, ¹*J* = 252.2 Hz); 163.99; 146.84; 137.71;
888 132.80 (d, ⁴*J* = 3.2 Hz); 131.04 (2C, d, ³*J* = 9.5 Hz); 121.75; 115.79 (2C, d, ²*J* = 21.9 Hz);
889 42.64; 38.44. Anal. Calc. for C₁₂H₁₀FN₃O₃: C 54.76%, H 3.83%, N 15.96%. Found: C 54.98%,
890 H 3.85%, N 15.82%.

891 *1-(4-chlorophenyl)-3-(4-nitro-1H-imidazol-1-yl)propan-1-one (2e)* Yield: 26%. Mp:
892 147.0-148.0 °C. IR (KBr) ν cm⁻¹: 1670 (s, ν_{C=O}), 1525 (s, ν_{NO₂}), 1336 (s, ν_{NO₂}). ¹H NMR
893 (DMSO-*d*₆, 400 MHz) δ ppm: 8.46 (d, 1H, **H₅**, $J_{5,2'} = 1.5$ Hz); 8.00 (d, 1H, **H₂ + H₆**, $J_{2,3} = J_{6,5} =$
894 8.6 Hz); 7.92 (d, 1H, **H_{2'}**, $J_{2',5'} = 1.4$ Hz); 7.62 (d, 2H, **H₃ + H₅**, $J_{3,2} = J_{5,6} = 8.5$ Hz); 4.43 (t, 2H,
895 **CH₂-N**, $J_{CH_2-CH_2} = 6.8$ Hz); 3.74 (t, 2H, **CH₂-CO**, $J_{CH_2-CH_2} = 6.8$ Hz). ¹³C NMR (DMSO-*d*₆, 100
896 MHz) δ ppm: 196.43; 146.84; 138.52; 137.70; 134.69; 129.91 (2C); 128.89 (2C); 121.74;
897 42.58; 38.51. Anal. Calc. for C₁₂H₁₀ClN₃O₃: C 51.53%, H 3.60%, N 15.02%. Found: C 51.37%,
898 H 3.51%, N 15.18%.

899 *1-(4-methoxyphenyl)-3-(4-nitro-1H-imidazol-1-yl)propan-1-one (3e)* Yield: 17%. Mp:
900 156.5-157.5 °C. IR (KBr) ν cm⁻¹: 1676 (s, ν_{C=O}), 1518 (s, ν_{NO₂}), 1330 (s, ν_{NO₂}). ¹H NMR
901 (DMSO-*d*₆, 400 MHz) δ ppm: 8.46 (d, 1H, **H₅**, $J_{5,2'} = 1.5$ Hz); 7.96 (d, 2H, **H₂ + H₆**, $J_{2,3} = J_{6,5} =$
902 9.0 Hz); 7.91 (d, 1H, **H_{2'}**, $J_{2',5'} = 1.5$ Hz); 7.05 (d, 2H, **H₃ + H₅**, $J_{3,2} = J_{5,6} = 8.9$ Hz); 4.41 (t, 2H,
903 **CH₂-N**, $J_{CH_2-CH_2} = 6.8$ Hz); 3.84 (s, 3H, **OCH₃**); 3.67 (t, 2H, **CH₂-CO**, $J_{CH_2-CH_2} = 6.8$ Hz). ¹³C
904 NMR (DMSO-*d*₆, 100 MHz) δ ppm: 195.65; 163.44; 146.83; 137.71; 130.34 (2C); 129.02;
905 121.76; 113.95 (2C); 55.58; 42.82; 38.11. Anal. Calc. for C₁₃H₁₃N₃O₄: C 56.72%, H 4.76%, N
906 15.27%. Found: C 56.55%, H 4.74%, N 15.72%.

907 *1-(benzo[b]thiophen-3-yl)-3-(4-nitro-1H-imidazol-1-yl)propan-1-one (4e)*. Yield: 21%.
908 Mp: 209.5-210.5 °C. IR (KBr) ν cm⁻¹: 1664 (s, ν_{C=O}), 1521 (s, ν_{NO₂}), 1324 (s, ν_{NO₂}). ¹H NMR
909 (DMSO-*d*₆, 400 MHz) δ ppm: 9.02 (s, 1H, **H₂**); 8.59 (dd, 1H, **H₅**, $J_{5,6} = 7.7$ Hz, $J_{5,8} = 1.3$ Hz);
910 8.49 (d, 1H, **H_{5'}**, $J_{5',2'} = 1.4$ Hz); 8.10 (d, 1H, **H₈**, $J_{8,7} = 7.4$ Hz); 7.94 (d, 1H, **H_{2'}**, $J_{2',4'} = 1.4$ Hz);
911 7.54-7.45 (m, 2H, **H₆+H₇**); 4.48 (t, 2H, **CH₂-N**, $J_{CH_2-CH_2} = 6.8$ Hz); 3.76 (t, 2H, **CH₂-CO**, $J_{CH_2-CH_2}$
912 = 6.8 Hz). ¹³C NMR (DMSO-*d*₆, 100 MHz) δ ppm: 192.76; 140.48; 139.37; 137.75; 136.02;
913 133.60; 125.91; 125.48; 124.57; 122.99; 121.78; 42.74; 39.84. Anal. Calc. for C₁₄H₁₁N₃O₃S: C
914 55.81%, H 3.68%, N 13.95%. Found: C 56.03%, H 3.57%, N 14.15%.

915 *1-(4-fluorophenyl)-3-(2-methyl-5-nitro-1H-imidazol-1-yl)propan-1-one (1f)*. Yield:
916 16%. Mp: 197.0-198.0 °C. IR (KBr) ν cm⁻¹: 1684 (s, ν_{C=O}), 1527 (s, ν_{NO₂}), 1388 (s, ν_{NO₂}). ¹H
917 NMR (DMSO-*d*₆, 400 MHz) δ ppm: 8.36 (s, 1H, **H_{4'}**); 8.08 (dd, 2H, **H₂ + H₆**, $J_{2,3} = J_{6,5} = 8.5$ Hz,
918 $J_{2,F} = J_{6,F} = 5.6$ Hz); 7.37 (t, 2H, **H₃ + H₅**, $J_{3,2} = J_{5,6} = 8.8$ Hz); 4.32 (t, 2H, **CH₂-N**, $J_{CH_2-CH_2} = 6.8$
919 Hz); 3.69 (t, 2H, **CH₂-CO**, $J_{CH_2-CH_2} = 6.8$ Hz); 2.43 (s, 3H, **CH₃-Amine**). ¹³C NMR (DMSO-*d*₆,
920 100 MHz) δ ppm: 196.01; 165.24 (d, ¹*J* = 251.7 Hz); 145.36; 132.83 (d, ⁴*J* = 2.9 Hz); 131.09
921 (2C, d, ³*J* = 9.7 Hz); 122.13 (2C); 115.78 (2C, d, ²*J* = 21.8 Hz); 41.62; 38.13; 12.69. Anal. Calc.
922 for C₁₃H₁₂FN₃O₃: C 56.32%, H 4.36%, N 15.16%. Found: C 56.39%, H 4.48%, N 15.18%.

923 *1-(4-chlorophenyl)-3-(2-methyl-5-nitro-1H-imidazol-1-yl)propan-1-one* (**2f**) Yield:
924 13%. Mp: 194.5-195.5 °C. IR (KBr) ν cm⁻¹: 1686 (s, $\nu_{C=O}$), 1568 (s, ν_{NO_2}), 1387 (s, ν_{NO_2}). ¹H
925 NMR (DMSO-*d*₆, 400 MHz) δ ppm: 8.35 (s, 1H, **H₄**); 8.01 (d, 2H, **H₂** + **H₆**, $J_{2-3} = J_{6-5} = 8.0$ Hz);
926 7.61 (d, 2H, **H₃** + **H₅**, $J_{3-2} = J_{5-6} = 8.2$ Hz); 4.32 (t, 2H, **CH₂-N**, $J_{CH_2-CH_2} = 6.8$ Hz); 3.69 (t, 2H,
927 **CH₂-CO**, $J_{CH_2-CH_2} = 6.8$ Hz); 2.43 (s, 3H, **CH₃-Amine**). ¹³C NMR (DMSO-*d*₆, 100 MHz) δ ppm:
928 196.45; 145.34; 138.50; 134.73; 129.96 (2C); 128.86 (2C); 122.13; 41.56; 38.22; 12.68. Anal.
929 Calc. for C₁₃H₁₂ClN₃O₃: C 53.16%, H 4.12%, N 14.31%. Found: C 53.16%, H 4.12%, N
930 14.31%.

931 *1-(4-methoxyphenyl)-3-(2-methyl-5-nitro-1H-imidazol-1-yl)propan-1-one* (**3f**) Yield:
932 23%. Mp: 139.5-140.5 °C. IR (KBr) ν cm⁻¹: 1678 (s, $\nu_{C=O}$), 1572 (s, ν_{NO_2}), 1391 (s, ν_{NO_2}). ¹H
933 NMR (DMSO-*d*₆, 400 MHz) δ ppm: 8.36 (s, 1H, **H₄**); 7.97 (d, 2H, **H₂** + **H₆**, $J_{2-3} = J_{6-5} = 8.9$ Hz);
934 7.05 (d, 2H, **H₃** + **H₅**, $J_{3-2} = J_{5-6} = 8.9$ Hz); 4.30 (t, 2H, **CH₂-N**, $J_{CH_2-CH_2} = 6.8$ Hz); 3.84 (s, 3H,
935 **OCH₃**); 3.62 (t, 2H, **CH₂-CO**, $J_{CH_2-CH_2} = 6.8$ Hz); 2.43 (s, 3H, **CH₃-Amine**). ¹³C NMR (DMSO-
936 *d*₆, 100 MHz) δ ppm: 195.69; 163.43; 145.34; 130.40 (2C); 129.05; 122.12; 113.93 (2C); 55.59;
937 41.79; 37.77; 12.69. Anal. Calc. for C₁₄H₁₅N₃O₄: C 58.13%, H 5.23%, N 14.53%. Found: C
938 58.30%, H 5.41%, N 14.70%.

939 *1-(benzo[b]thiophen-3-yl)-3-(2-methyl-5-nitro-1H-imidazol-1-yl)propan-1-one* (**4d**).
940 Yield: 21%. Mp: 113.0-114.0 °C. IR (KBr) ν cm⁻¹: 1666 (s, $\nu_{C=O}$), 1528 (s, ν_{NO_2}), 1392 (s, ν_{NO_2}).
941 ¹H NMR (DMSO-*d*₆, 400 MHz) δ ppm: 9.03 (s, 1H, **H₂**); 8.60 (d, 1H, **H₅**, $J_{5-6} = 7.9$ Hz); 8.39 (s,
942 1H, **H₄**); 8.09 (d, 1H, **H₈**, $J_{8-7} = 7.8$ Hz); 7.49 (dt, 1H, **H₆** + **H₇**, $J_{6-5} = J_{7-8} = 21.5$, Hz $J_{6-7} = J_{7-6} =$
943 7.1 Hz); 4.37 (t, 2H, **CH₂-N**, $J_{CH_2-CH_2} = 6.9$ Hz); 3.72 (t, 2H, **CH₂-CO**, $J_{CH_2-CH_2} = 6.9$ Hz); 2.45 (s,
944 3H, **CH₃-Amine**). ¹³C NMR (DMSO-*d*₆, 100 MHz) δ ppm: 192.76; 145.36; 145.33; 140.46;
945 139.34; 136.02; 133.62; 125.89; 125.45; 124.56; 122.97; 122.11; 41.71; 39.45; 12.69. Anal.
946 Calc. for C₁₅H₁₃N₃O₃S: C 57.13%, H 4.16%, N 13.33%. Found: C 57.26%, H 4.02%, N 10.32%.

947 *1-(4-fluorophenyl)-3-(5-methyl-4-nitro-1H-imidazol-1-yl)propan-1-one* (**1g**). Yield:
948 16%. Mp: 140.5-141.5 °C. IR (KBr) ν cm⁻¹: 1678 (s, $\nu_{C=O}$), 1535 (s, ν_{NO_2}), 1353 (s, ν_{NO_2}). ¹H
949 NMR (DMSO-*d*₆, 400 MHz) δ ppm: 8.08 (dd, 2H, **H₂** + **H₆**, $J_{2-3} = J_{6-5} = 8.2$ Hz, $J_{2-F} = J_{6-F} = 5.7$
950 Hz); 7.82 (s, 1H, **H_{2'}**); 7.37 (t, 2H, **H₃** + **H₅**, $J_{3-2} = J_{5-6} = 8.8$ Hz); 4.37 (t, 2H, **CH₂-N**, $J_{CH_2-CH_2} =$
951 6.7 Hz); 3.64 (t, 2H, **CH₂-CO**, $J_{CH_2-CH_2} = 6.8$ Hz); 2.63 (s, 3H, **CH₃-Amine**). ¹³C NMR (DMSO-
952 *d*₆, 100 MHz) δ ppm: 195.93; 165.22 (d, ¹ $J = 252.2$ Hz); 143.78; 135.93; 132.82 (d, ⁴ $J = 2.9$
953 Hz); 131.94; 131.07 (2C, d, ³ $J = 9.5$ Hz); 115.76 (2C, d, ² $J = 21.8$ Hz); 40.26; 38.04; 10.16.
954 Anal. Calc. for C₁₃H₁₂FN₃O₃: C 56.32%, H 4.36%, N 15.16%. Found: C 56.31%, H 4.30%, N
955 15.22%.

956 *1-(4-chlorophenyl)-3-(5-methyl-4-nitro-1H-imidazol-1-yl)propan-1-one* (**2g**) Yield:
957 15%. Mp: 164.5-165.5 °C. IR (KBr) ν cm⁻¹: 1686 (s, $\nu_{C=O}$), 1566 (s, ν_{NO_2}), 1342 (s, ν_{NO_2}). ¹H
958 NMR (DMSO-*d*₆, 400 MHz) δ ppm: 7.99 (d, 2H, **H₂** + **H₆**, $J_{2-3} = J_{6-5} = 8.6$ Hz); 7.81 (s, 1H, **H_{2'}**);
959 7.61 (d, 2H, **H₃** + **H₅**, $J_{3-2} = J_{5-6} = 8.6$ Hz); 4.36 (t, 2H, **CH₂-N**, $J_{CH_2-CH_2} = 6.8$ Hz); 3.64 (t, 2H,

960 **CH₂-CO**, $J_{CH_2-CH_2} = 6.8$ Hz); 2.63 (s, 3H, **CH₃-Amine**). ¹³C NMR (DMSO-*d*₆, 100 MHz) δ ppm:
961 196.37; 143.78; 138.48; 135.93; 134.72; 131.94; 129.95 (2C); 128.84 (2C); 40.21; 38.12; 10.16.
962 Anal. Calc. for C₁₃H₁₂ClN₃O₃: C 53.16%, H 4.12%, N 14.31%. Found: C 53.14%, H 4.27%, N
963 14.26%.

964 *1-(4-methoxyphenyl)-3-(5-methyl-4-nitro-1H-imidazol-1-yl)propan-1-one (3g)* Yield:
965 27%. Mp: 149.0-150.0 °C. IR (KBr) ν cm⁻¹: 1682 (s, ν_{C=O}), 1565 (s, ν_{NO₂}), 1403 (s, ν_{NO₂}). ¹H
966 NMR (DMSO-*d*₆, 400 MHz) δ ppm: 7.97 (d, 2H, **H₂ + H₆**, $J_{2-3} = J_{6-5} = 8.9$ Hz); 7.82 (s, 1H, **H₇**);
967 7.05 (d, 2H, **H₃ + H₅**, $J_{3-2} = J_{5-6} = 8.9$ Hz); 4.35 (t, 2H, **CH₂-N**, $J_{CH_2-CH_2} = 6.8$ Hz); 3.85 (s, 3H,
968 **OCH₃**); 3.58 (t, 2H, **CH₂-CO**, $J_{CH_2-CH_2} = 6.8$ Hz); 2.64 (s, 3H, **CH₃-Amine**). ¹³C NMR (DMSO-
969 *d*₆, 100 MHz) δ ppm: 195.60; 163.42; 143.76; 135.93; 131.92; 130.38 (2C); 129.03; 113.92
970 (2C); 55.59; 40.42; 37.68; 10.16. Anal. Calc. for C₁₄H₁₅N₃O₄: C 58.13%, H 5.23%, N 14.53%.
971 Found: C 58.44%, H 5.40%, N 14.49%.

972 *1-(benzo[b]thiophen-3-yl)-3-(5-methyl-4-nitro-1H-imidazol-1-yl)propan-1-one (4g)*.
973 Yield: 16%. Mp: 180.0-181.0 °C. IR (KBr) ν cm⁻¹: 1662 (s, ν_{C=O}), 1568 (s, ν_{NO₂}), 1342 (s, ν_{NO₂}).
974 ¹H NMR (DMSO-*d*₆, 400 MHz) δ ppm: 9.01 (s, 1H, **H₂**); 8.61 (d, 1H, **H₅**, $J_{5-6} = 7.8$ Hz); 8.09 (d,
975 1H, **H₈**, $J_{8-7} = 7.8$ Hz); 7.85 (s, 1H, **H₇**); 7.49 (dtd, 1H, **H₆ + H₇**, $J_{6-5} = J_{7-8} = 15.2$, Hz $J_{6-7} = J_{7-6} =$
976 7.1 Hz, $J_{6-2} = J_{7-2} = 5.8$ Hz); 4.42 (t, 2H, **CH₂-N**, $J_{CH_2-CH_2} = 6.9$ Hz); 3.67 (t, 2H, **CH₂-CO**, $J_{CH_2-CH_2}$
977 $= 6.9$ Hz); 2.65 (s, 3H, **CH₃-Amine**). ¹³C NMR (DMSO-*d*₆, 100 MHz) δ ppm: 192.68; 143.81;
978 140.43; 139.33; 136.03; 135.95; 133.61; 131.87; 125.89; 125.45; 124.56; 122.97; 40.35; 40.19;
979 10.18. Anal. Calc. for C₁₅H₁₃N₃O₃S: C 57.13%, H 4.16%, N 13.33%. Found: C 57.53%, H
980 3.74%, N 13.12%.

981

982 **4.4 Compound Handling**

983 Stocks of the synthesised compounds and the reference drug BZ (Sigma-Aldrich) were prepared
984 in 100% DMSO at 50 mM in eppendorf tubes, and stored at 4°C. Working stocks were prepared
985 in culture medium on the same day as the assay. At final concentration, all the sample wells for
986 the assay contained <0.5% of DMSO. All plates were inspected microscopically to detect
987 contamination or precipitation of the compounds.

988

989 **4.5 Parasite and Mammalian Cell Cultures**

990 *T. cruzi* CL-Luc:Neon clone parasites (a bioluminescent:fluorescent derivative of the CL-Brener
991 clone – DTU-VI) were cultured in supplemented RPMI-1640 medium, as described previously
992 [27]. BSR cells (BHK-21 subclone) were cultured in Dulbecco's Modified Eagle's Medium
993 (DMEM, Sigma) supplemented with 5% (v/v) Foetal Bovine Serum (FBS), 100 U/ml of
994 penicillin, and 100 µg/ml streptomycin at 37°C and 5% CO₂. For maintenance, BSR cells were
995 sub-cultured every 3 days at a ratio of 1:5. For the infection of cell monolayers, tissue culture

996 trypomastigotes (TCTs) were derived from previously infected BSR cells. Cell cultures were
997 exposed to TCTs for 18 h (overnight). Extracellular parasites were then removed by washing
998 with PBS, and the flasks incubated with fresh medium for a further 5–7 days. New extracellular
999 TCTs were isolated by collection and centrifugation of the culture medium at 1600 g. Pellets
1000 were re-suspended in DMEM with 10% of FBS and kept at 37°C until use. Motile
1001 trypomastigotes were counted using a haemocytometer.

1002 **4.6 Biological Assays**

1003 *4.6.1 Data analysis and definitions*

1004 Fluorescence intensities were determined using a BMG FLUOstar Omega (with excitation 488
1005 nm, emission 525 nm for the fluorescent parasites and excitation 530 nm, emission 595 nm for
1006 the Alamar blue® assays). Dose-response curves were fitted and 95% confidence intervals were
1007 calculated using the sigmoidal dose-response variable slope function from the Graph Pad Prism
1008 8 software (La Jolla California USA, www.graphpad.com). In this study: i) % inhibition of
1009 growth is the reduction in the replication rate in the presence of the drug with respect to the
1010 untreated controls; ii) IC₅₀ is defined as the compound concentration capable of reducing the
1011 replication and/or infection by 50% as compared to non-treated controls and values were
1012 determined by interpolation from the fitted dose-response curve. Values are expressed as IC₅₀ ±
1013 SD; iii) selectivity index (SI) is an indicator of the specificity of growth inhibition of the
1014 parasite by the drug, in relation to its inhibition of the host cell; it was calculated as the ratio of
1015 host cell:parasite IC₅₀ values. For the comet assay, the mean DNA in the tail for each condition
1016 was compared with the vehicle control value using the Kruskal-Wallis test followed, if needed,
1017 by the post-hoc Bonferroni test. Statistical significance was set at p<0.05 in both tests. The
1018 Statistics and Data Analysis (STATA) software v12.1 (TX, USA) was used. All determinations
1019 were performed in 3 independent experiments with 3 technical replicates per concentration,
1020 unless stated otherwise.

1021

1022 *4.6.2 In vitro pre-screening assays*

1023 Single-point potency assays of 10 μM and 40 μM of drug for epimastigotes and BSR cells,
1024 respectively, were set for 72 h exposure. The activity of the drugs was measured by adding
1025 0.125 μg/ml of Alamar Blue® (AB, Laboserv, Giessen, Germany) [38]. AB is reduced by the
1026 organisms in a time-dependent process, and plates were incubated for 24 h in the case of the
1027 epimastigotes and 6 h in the case of the BSR cells. These incubation times were standardised in
1028 our lab, as they depend on the initial plating concentration of the untreated controls. After

1029 incubation, the plates were read at 540 nm. A linear relationship between cellular density and
1030 absorbance can be used to determine the growth.

1031 Epimastigotes of *T. cruzi* CL-Luc:Neon clone were seeded at 2.5×10^5 parasites per well in 96
1032 well plates in 100 μL of culture medium. To these was added another 100 μL of medium
1033 containing 20 μM of drug, to reach a final concentration of 10 μM in the assay. Plates were then
1034 incubated at 27°C for 72 h before addition of AB. BSR cells were seeded at 5×10^4 cells per
1035 well in 96 well plates in 100 μL of culture medium and allowed to adhere for 6 h at 37°C and
1036 5% CO_2 . Then, another 100 μL medium containing 80 μM drug was added for a final
1037 concentration of 40 μM in the assay. The plates were then incubated for an additional 72 h
1038 before addition of AB.

1039

1040 *4.6.3 In vitro screening and selectivity index*

1041 8-point potency curves were generated by serial dilution (2:1) of the drugs in the corresponding
1042 culture medium. For epimastigote and BSR cell screening, the seeding and incubation was
1043 performed as above for the pre-screenings. For amastigote assays, BSR cells in 100 μL growth
1044 medium were added to a black, clear-bottomed, 96-well, lidded, polystyrene microplate at $5 \times$
1045 10^4 cells/well. After 6 h incubation to allow attachment, cells were infected overnight with $5 \times$
1046 10^5 TCT/well, a multiplicity of infection (MOI) of 10. The trypomastigote to mammalian cell
1047 ratios used were determined empirically, as the minimum ratio necessary to achieve optimal
1048 infection levels is statistically distinguishable from background. Next day, wells were washed 3
1049 times with PBS to remove non-internalised trypomastigotes, before adding 200 μL DMEM
1050 supplemented with 1% FBS and containing the drugs at the different concentrations. For
1051 assessment of activity against amastigote replication, 72 h post-incubation, the plates were
1052 washed twice with PBS and fixed with 4% paraformaldehyde for 30 min. Then,
1053 paraformaldehyde was removed, and wells washed with PBS, before taking a fluorescence
1054 readout in the BMG FLUOstar Omega plate reader. For trypomastigote screening assays,
1055 infective TCTs were isolated from a previously infected culture flask and incubated in
1056 eppendorf tubes with the different drug concentrations for 6 h in high-glucose DMEM,
1057 supplemented with 10% FBS, at 37°C. Then, trypomastigotes were washed 3 times with PBS to
1058 remove the drug from the medium, and used to infect a plate seeded with BSR cells as above.
1059 Non-internalised parasites were removed from the medium on the following day by washing the
1060 plates 3 times with PBS, and 200 μL fresh growth medium supplemented with 1% FBS was
1061 added. Infection was allowed to progress for an additional 72 h. For assessment of activity
1062 against trypomastigotes, we measured the reduction of cell-invasion by quantifying fluorescence

1063 generated by amastigote replication upon successful infection. IC₅₀ values were calculated using
1064 the Graph Pad Prism 8 software as explained above

1065

1066 *4.6.4 Kinetics of killing*

1067 Changes in the fluorescence intensity were assessed by daily readouts using the plate reader. For
1068 this assay, epimastigotes were seeded as above in 96-well microplates. Growth curves were
1069 monitored during the 5 days of exponential growth in the presence of the compounds, until the
1070 parasites reached stationary phase (around day 5 after plating). BZ was included as a ‘fast-
1071 killing’ drug control.

1072

1073 *4.6.5 Wash-out assays*

1074 *In vitro* infections were carried out as above. However, BSR cells were seeded in 8-well, Ibidi
1075 μ -slides with a polymer coverslip, (Cat. No: 80826) or in black, clear-bottomed, 24-well, lidded
1076 polystyrene microplates. The concentrations used in these assays were 10x and 20x the IC₅₀
1077 value obtained previously for the amastigote form. Infections were divided into two groups for
1078 each concentration under study. One group was exposed to the drug for 10 days, while the other
1079 group was exposure to the drug for 20 days. Compounds were replaced every 4 days. Relapse
1080 day was defined as the first day trypomastigotes could be observed by light microscopy in
1081 culture after wash-out of the drug, or replication of amastigotes was observed by fluorescence
1082 microscopy. Three wells were prepared per treatment and each individual well was inspected by
1083 taking 30 captures per timepoint. These assays allow drugs to be assessed as trypanocidal or
1084 trypanostatic.

1085 Images were acquired using an inverted Nikon Eclipse microscope. The chamber/plate
1086 containing the infected cells was moved along the x-y plane through a 580 nm LED
1087 illumination. Images were collected using a 16-bit, 1-megapixel Pike AVT (F-100B) CCD
1088 camera set in the detector plane. An Olympus LMPlanFLN 40x/1.20 objective was used to
1089 collect the exit wave leaving the specimen. Imaging was performed by placing the chamber
1090 slide/plate on a microscope surrounded by an environmental chamber (OKOLab cage incubator,
1091 USA) maintaining the cells and the microscope at 37°C and 5% CO₂. Sequences were created
1092 using the deconvolution app in Nikon imaging software.

1093

1094 *4.6.6 Infectivity assays*

1095 This assay is a variation of the trypomastigote screening procedure used to determine the
1096 efficacy of drugs in preventing infection, either by killing the parasite directly, or by affecting
1097 the fitness of the parasite, and blocking infection. Briefly, trypomastigotes are incubated for 6 h
1098 in serial drug concentrations, then parasites were washed 3 times with PBS and used to infect
1099 the BSR mammalian cells at a MOI of 10:1 (trypomastigote:cell) for 18 h. This allows the
1100 concentration that prevents establishment of a productive infection to be determined. Infected
1101 BSR cells were readout 120 h post-infection, and chambers were inspected for amastigote
1102 replication using an inverted Nikon Eclipse microscope, as explained above.

1103

1104 *4.6.7 Drug combination assays*

1105 To test drug combinations, the Alamar Blue and fluorescence methods were used to determine
1106 the IC₅₀ values. Parasites/cells were seeded in the previously described conditions, but the BZ
1107 IC₅₀ values were re-evaluated in the presence of the IC₅₀ of the drug under study. Drug
1108 combinations were assessed in triplicate in each plate and repeated at least twice. The
1109 combination index (CI) isobologram method was used to analyse the nature of the interaction
1110 [39]. A Ci value less than, equal to, or greater than 1 indicates synergism, additivity, and
1111 antagonism, respectively.

1112

1113 **4.7 Comet Assay**

1114 *4.7.1 Cell culture*

1115 TK-6 cells (human lymphoblastoid cell line) were obtained from the American Type Culture
1116 Collection (ATCC). They were grown in RPMI 1640 medium (ATCC modification, ref.
1117 A1049101) supplemented with 10% FBS, 100 U/mL penicillin and 0.1 mg/mL streptomycin (all
1118 from Gibco). Cells were maintained as a suspension culture in continuous agitation at 37 °C in a
1119 humidified atmosphere with 5% CO₂ for no longer than 60 days.

1120 *4.7.2 Cell treatment*

1121 1 mL containing 6 x 10⁵ TK-6 cell suspension was treated with compound **3c** in a 12-well plate,
1122 for 3 h. The treatment was performed in the cell culture medium. After that, cells were washed
1123 three times in, and then suspended in 1.5 mL of fresh cell culture medium. 0.5 mL of cell
1124 suspension was used for analysis and 1 mL for the proliferation assay (**below**). Cells treated
1125 with 20 μM MMS were used as a positive control for the Fpg-modified comet assay. Three
1126 independent experiments were performed.

1127

1128 *4.7.3 Proliferation assay*

1129 After cell treatment and wash, cells were resuspended in fresh culture medium and incubated for
1130 48 h, with continuous agitation at 37°C in a humidified atmosphere with 5% CO₂. Cells were
1131 counted after 24 h, to adjust the cell concentration, and again at 48 h. The total suspension
1132 growth (TSG) was calculated by dividing the number of cells after 48 h by the number of cells
1133 just before treatment. Relative suspension growth (RSG) is the relation between the TSG of
1134 each treated cell suspension and the TSG of the control cells, expressed as a percentage.

1135

1136 *4.7.4 FPG-modified comet assay*

1137 The comet assay was carried out using the 12 minigels/slide format and the 12-Gel Comet
1138 Assay Units (Norgenotech, Norway) [40,41]. Treated cells were embedded in agarose by
1139 mixing 30 µL of cell suspension with 140 µL of 1% low-melting-point agarose in PBS at 37°C.
1140 Six 5 µL aliquots, 2 per condition tested, were placed on agarose-pre-coated microscope slides.
1141 Slides were immersed in lysis solution (2.5 M NaCl, 0.1 M Na₂EDTA, 0.1 M Tris, pH 10, 1%
1142 Triton X-100) for 1 h at 4°C, and then three times, 5 min each, in Fpg reaction buffer (40 mM
1143 HEPES, 0.1 M KCl, 0.5 mM EDTA, 0.2 mg/mL BSA, pH 8.0). Each condition (two gels)
1144 involved incubation at 37°C for 1 hour with 30 µL of either lysis buffer (without Triton X-100),
1145 enzyme reaction buffer, or Fpg. Slides were then immersed in the electrophoresis solution (0.3
1146 M NaOH, 1 mM Na₂EDTA, pH >13) for 40 min at 4°C and electrophoresis was carried out at
1147 1.2 V/cm for an additional 20 min. Slides were then immersed sequentially in DPBS and
1148 distilled water for 10 min each, and in 70% and 100% ethanol, 15 min each, before drying
1149 overnight.

1150 Comets were stained by adding a drop of 1 µg/mL 4,6-diamidino-2-phenylindole (DAPI) to
1151 each mini-gel. The semi-automated image analysis system Comet Assay IV (Perceptive
1152 Instruments) was used to measure the percentage of tail DNA of 50 comets per gel (100 comets
1153 per condition). The median percentage of DNA in the tail for 100 comets was the descriptor of
1154 each condition; gels incubated with the lysis solution (without Triton X-100) represents SBs and
1155 alkali labile sites (ALS), and net Fpg-sensitive sites were calculated by subtracting the values in
1156 the enzyme reaction buffer from those obtained after the Fpg incubation.

1157

1158 **ACKNOWLEDGEMENTS**

1159 IB-H is grateful to Fundación Caja Navarra, Obra Social la Caixa, Fundación Roviralta, Grupo
1160 Ubesol and Inversiones Garcilaso de la Vega for their financial support. Moreover, IB-H is
1161 grateful to the ISTUN Instituto de Salud Tropical of the Universidad de Navarra for their grant.
1162

1163 REFERENCES

- 1164 [1] WHO. Chagas disease (American trypanosomiasis).
1165 <https://www.who.int/chagas/disease/en/> (accessed 12 December 2019).
- 1166 [2] DNDi. Diseases & Projects. About Chagas disease. [https://www.dndi.org/diseases-](https://www.dndi.org/diseases-projects/chagas/)
1167 [projects/chagas/](https://www.dndi.org/diseases-projects/chagas/) (accessed 12 December 2019).
- 1168 [3] C. Bern, Chagas' Disease, N. Engl. J. Med. 373 (2015) 456-466.
- 1169 [4] J. Bermudez, C. Davies, A. Simonazzi, J. Pablo Real, S. Palma, Current drug therapy
1170 and pharmaceutical challenges for Chagas disease, Acta Trop. 156 (2016) 1-16.
- 1171 [5] R. Paucar, E. Moreno-Viguri, S. Pérez-Silanes, Challenge in Chagas Disease Drug
1172 Discovery: A Review, Curr. Med. Chem. 23 (2016) 3154-3170.
- 1173 [6] I. Beltran-Hortelano, S. Perez-Silanes, S. Galiano, Trypanothione Reductase and
1174 Superoxide Dismutase as Current Drug Targets for Trypanosoma cruzi: An Overview of
1175 Compounds with Activity against Chagas Disease, Curr. Med. Chem. 24 (2017) 1066-1138.
- 1176 [7] S. Bala, N. Sharma, A. Kajal, S. Kamboj, V. Saini, Mannich bases: an important
1177 pharmacophore in present scenario, Int. J. Med. Chem. (2014) 191072.
- 1178 [8] G. Roman, Mannich bases in medicinal chemistry and drug design, Eur. J. Med. Chem.
1179 89 (2015) 743-816.
- 1180 [9] I.N. Wenzel, P.E. Wong, L. Maes, T.J. Müller, R.L. Krauth-Siegel, M.P. Barret, E.
1181 Davioud-Charvet E, Unsaturated Mannich bases active against multidrug-resistant
1182 *Trypanosoma brucei brucei* strains, Chem. Med. Chem. 4 (2009) 339-351.
- 1183 [10] V.M. Patel, N.B. Patel, M.J. Chan-Bacab, G. Rivera, Synthesis, biological evaluation
1184 and molecular dynamics studies of 1,2,4-triazole clubbed Mannich bases, Comput. Biol. Chem.
1185 76 (2018) 264-274.
- 1186 [11] I. Al Nasr, J. Jentzsch, I. Winter, R. Schobert, K. Ersfeld, W.S. Koko, A.A.H. Mujawah,
1187 T.A. Khan, B. Biersack, Antiparasitic activities of new lawsone Mannich bases, Arch. Pharm.
1188 (Weinheim) 352 (2019) e1900128.
- 1189 [12] A. Martín-Montes, M. Santivañez-Veliz, E. Moreno-Viguri, R. Martín-Escolano, C.
1190 Jiménez-Montes, C. Lopez-Gonzalez, C. Marín, C. Sanmartín, R. Gutiérrez Sánchez, M.
1191 Sánchez-Moreno, S. Pérez-Silanes, *In vitro* antileishmanial activity and iron superoxide
1192 dismutase inhibition of arylamine Mannich base derivatives, Parasitology 144 (2017) 1783-
1193 1790.

1194 [13] B.M. Kotecka, G.B. Barlin, M.D. Edstein, K.H. Rieckmann, New quinoline di-Mannich
1195 base compounds with greater antimalarial activity than chloroquine, amodiaquine, or
1196 pyronaridine, *Antimicrob. Agents Chemother.* 41 (1997) 1369-1374.

1197 [14] K.J. Raynes, P.A. Stocks, P.M. O'Neill, B.K. Park, S.A. Ward, New 4-aminoquinoline
1198 Mannich base antimalarials. 1. Effect of an alkyl substituent in the 5'-position of the 4'-
1199 hydroxyanilino side chain. *J. Med. Chem.* 42 (1999) 2747-2751.

1200 [15] Y. Li, Z.S. Yang, H. Zhang, B.J. Cao, F.D. Wang, Y. Zhang, Y.L Shi, J.D. Yang, B.A.
1201 Wu, Artemisin derivatives bearing Mannich base group: synthesis and antimalarial activity,
1202 *Bioorg. Med. Chem.* (2003) 4363-4368.

1203 [16] J. Okombo, C. Brunschwig, K. Singh, G.A. Dziwornu, L. Barnard, M. Njoroge, S.
1204 Wittlin, K. Chibale, Antimalarial Pyrido [1,2-a]benzimidazole Derivatives with Mannich Base
1205 Side Chains: Synthesis, Pharmacological Evaluation, and Reactive Metabolite Trapping Studies,
1206 *ACS Infect. Dis.* 5 (2019) 372-384.

1207 [17] E. Moreno-Viguri, C. Jiménez-Montes, R. Martín-Escolano, M. Santivañez-Veliz, A.
1208 Martín-Montes, A. Azqueta, M. Jimenez-Lopez, S. Zamora Ledesma, N. Cirauqui, A. López de
1209 Cerain, C. Marín, M. Sánchez-Moreno, S. Pérez-Silanes, *In vitro* and *in Vivo* Anti-
1210 *Trypanosoma cruzi* Activity of New Arylamine Mannich Base-Type Derivatives, *J. Med.*
1211 *Chem.* 59 (2016) 10929-10945.

1212 [18] R. Martín-Escolano, E. Moreno-Viguri, M. Santivañez-Veliz, A. Martín-Montes, E.
1213 Medina-Carmona, R. Paucar, C. Marín, A. Azqueta, N. Cirauqui, A.L. Pey, S. Pérez-Silanes, M.
1214 Sánchez-Moreno, Second Generation of Mannich Base-Type Derivatives with *in Vivo* Activity
1215 against *Trypanosoma cruzi*, *J. Med. Chem.* 61 (2018) 5643-5663.

1216 [19] R. Paucar, R. Martín-Escolano, E. Moreno-Viguri, N. Cirauqui, C. Rangel Rodrigues,
1217 C. Marín, M. Sánchez-Moreno, S. Pérez-Silanes, M. Ravera, E. Gabano, A step towards
1218 development of promising trypanocidal agents: Synthesis, characterization and *in vitro*
1219 biological evaluation of ferrocenyl Mannich base-type derivatives, *Eur. J. Med. Chem.* 163
1220 (2019) 569-582.

1221 [20] R. Paucar, R. Martín-Escolano, E. Moreno-Viguri, A. Azqueta, N. Cirauqui, C. Marín,
1222 M. Sánchez-Moreno, S. Pérez-Silanes. Rational modification of Mannich base-type derivatives
1223 as novel antichagasic compounds: Synthesis, *in vitro* and *in vivo* evaluation. *Bioorg. Med.*
1224 *Chem.* 27 (2019) 3902-3917.

1225 [21] J. Alonso-Padilla, I. Cotillo, J.L. Presa, J. Cantizani, I. Peña, A.I. Bardera, J.J. Martín,
1226 A. Rodriguez, Automated High-Content Assay for Compounds Selectively Toxic to
1227 *Trypanosoma cruzi* in a Myoblastic Cell Line, *PLoS Negl. Trop. Dis.* 9 (2015) e0003493.

1228 [22] M.L. Sykes, V.M. Avery, Development and application of a sensitive, phenotypic, high-
1229 throughput image-based assay to identify compound activity against *Trypanosoma cruzi*
1230 amastigotes, *Int. J. Parasitol. Drugs Drug Resist.* 5 (2015) 215-228.

1231 [23] M. De Ricker, J. Thomas, J. Riley, S.J. Brough, T.J. Miles, D.W. Gray, Identification of
1232 Trypanocidal Activity for Known Clinical Compounds Using a New *Trypanosoma cruzi* Hit-
1233 Discovery Screening Cascade, *PLoS Negl. Trop. Dis.* 10 (2016) e0004584.

1234 [24] L.M. MacLean, J. Thomas, M.D. Lewis, I. Cotillo, D.W. Gray, M. De Ricker,
1235 Development of *Trypanosoma cruzi in vitro* assays to identify compounds suitable for
1236 progression in Chagas' disease drug discovery, *PLoS Negl. Trop. Dis.* 12 (2018) e0006612.

1237 [25] I. Beltran-Hortelano, V. Alcolea, M. Font, S. Pérez-Silanes, The role of imidazole and
1238 benzimidazole heterocycles in Chagas disease: A review, *Eur. J. Med. Chem.* 206 (2020)
1239 112692. DOI: 10.1016/j.ejmech.2020.112692.

1240 [26] A. Bugarin, K.D. Jones, B.T. Connel, Efficient, direct α -methylation of carbonyls
1241 mediated by diisopropylammonium trifluoroacetate, *Chem. Commun.* 46 (2010) 1715-1717.

1242 [27] F.C. Costa, A.F. Francisco, S. Jayawardhana, S.G. Calderano, M.D. Lewis, F. Olmo, T.
1243 Beneke, E. Gluenz, J. Sunter, S. Dean, J.M. Kelly, M.C. Taylor, Expanding the toolbox for
1244 *Trypanosoma cruzi*: A parasite line incorporating a bioluminescence-fluorescence dual reporter
1245 and streamlined CRISPR/Cas9 functionality for rapid *in vivo* localisation and phenotyping,
1246 *PLoS Negl. Trop. Dis.* 12 (2018) e0006388.

1247 [28] Bustamante JM, Sanchez-Valdez F, Padilla AM, White B, Wang W, Tarleton RL. A
1248 modified drug regimen clears active and dormant trypanosomes in mouse models of Chagas
1249 disease, *Sci Transl Med.* 12(567) (2020) eabb7656.

1250 [29] S. Agnihotri, R. Narula, K. Joshi, S. Rana, M. Singh, *In silico* modeling of ligand
1251 molecule for non structural 3 (NS3) protein target of flaviviruses, *Bioinformation* 8 (2012) 123-
1252 127.

1253 [30] T. Sander, J. Freyss, M. von Korff, J.R. Reich, C. Rufener, OSIRIS, an entirely in-house
1254 developed drug discovery informatics system, *J. Chem. Infect. Model.* 49 (2009) 232-246.

1255 [31] L.Z. Benet, C.M. Hosey, O. Ursu, T.I. Oprea, BDDCS, the rule of 5 and Drugability,
1256 *Adv. Drug Deliv. Rev.* 101 (2016).

1257 [32] C. Hundsdorfer, H.J. Hemmerling, J. Hamberger, M. Le Borgne, P. Bednarski, C. Gotz,
1258 F. Totzke, J. Jose, Novel indeno [1,2-*b*]indoloquinones as inhibitors of the human protein kinase
1259 CK2 with antiproliferative activity towards a broad panel of cancer cell lines. *Biochem.*
1260 *Biophys. Res. Commun.* 424 (2012) 749-756.

1261 [33] A.R. Ali, E.R. El-Bendary, M.A. Ghaly, I.A. Shehata, Novel acetamidothiazole
1262 derivatives: synthesis and *in vitro* anticancer evaluation, *Eur. J. Med. Chem.* 69 (2013) 908-919.

1263 [34] M. Cal, J.R. Ioset, M.A. Fügi, P. Mäser, M. Kaiser, Assessing anti-*T.cruzi* candidates *in*
1264 *vitro* for sterile cidality, *Int. J. Parasitol. Drugs Drug Resist.* 6 (2016) 165-170.

- 1265 [35] R.B. da Silva, V.B. Loback, K. Salomão, S.L. de Castro, J.L. Wardell, S.M. Wardell,
1266 T.E. Costa, C. Penido, M.d. Henriques, S.A. Carvalho, E.F. da Silva, C.A. Fraga, Synthesis and
1267 Trypanocidal Activity of Novel 2,4,5-Triaryl-*N*-Hydroxylimidazole Derivatives, *Molecules* 18
1268 (2013) 3445-3457.
- 1269 [36] A. Azqueta, A.R. Collins, The essential comet assay: a comprehensive guide to
1270 measuring DNA damage and repair, *Arch. Toxicol.* 87 (2013) 94-968.
- 1271 [37] G. Speit, P. Schutz, I. Bonzheim, K. Trenz, H. Hoffmann, Sensitivity of the FPG protein
1272 towards alkylation damage in the comet assay, *Toxicol. Lett.* 146 (2004) 151-158.
- 1273 [38] J. Mikus, D. Steverding, A simple colorimetric method to screen drug cytotoxicity
1274 against *Leishmania* using the dye Alamar Blue, *Parasitol. Int.* 48 (2003) 265-269.
- 1275 [39] T. Chou, Drug combination studies and their synergy quantification using the Chou-
1276 Talalay method, *Cancer Res.* 70 (2010) 440-446.
- 1277 [40] S. Shaposhnikov, A. Azqueta, S. Henriksson, S. Meier, I. Gaivao, N.H. Huskisson, A.
1278 Smart, G. Brunborg, M. Nilsson, A.R. Collins, Twelve-gel slide format optimized for comet
1279 assay and fluorescent *in situ* hybridization, *Toxicol. Lett.* 195 (2010) 31-34.
- 1280 [41] D. Muruzabal, S.A.S. Langie, B. Pourrut, A. Azqueta, The enzyme-modified comet
1281 assay: Enzyme incubation step in 2 vs 12-gels/slide systems, *Mutat. Res. – Genet. Toxicol.*
1282 *Environ. Mutagen.* 845 (2019) 402981.